Stochastic Inventory Management for Tactical Process Planning Under Uncertainties: MINLP Models and Algorithms

Fengqi You and Ignacio E. Grossmann
Dept. of Chemical Engineering, Carnegie Mellon University, Pittsburgh, PA 15213

DOI 10.1002/aic.12338
Published online August 12, 2010 in Wiley Online Library (wileyonlinelibrary.com).

We address in this article the mid-term planning of chemical complexes with integration of stochastic inventory management under supply and demand uncertainty. By using the guaranteed service approach to model time delays in the flows inside the network, we capture the stochastic nature of the supply and demand variations, and develop an equivalent deterministic optimization model to minimize the production, feedstock purchase, cycle inventory, and safety stock costs. The model determines the optimal purchases of the feedstocks, production levels of the processes, sales of final products, and safety stock levels of all the chemicals. We formulate the model as a mixed-integer nonlinear program with a nonconvex objective function and nonconvex constraints. To solve the global optimization problem with modest computational times, we exploit some model properties and develop a tailored branch-and-refine algorithm based on successive piecewise linear approximation. Five industrial-scale examples with up to 38 processes and 28 chemicals are presented to illustrate the application of the model and the performance of the proposed algorithm. © 2010 American Institute of Chemical Engineers *AIChE J,* 57: 1250–1277, 2011

Keywords: tactical planning, MINLP, stochastic inventory control, chemical process network

Introduction

The chemical process industry often constructs large production sites, namely, integrated chemical complexes[1–3] that are composed of many interconnected processes and various chemicals. The integrated chemical complexes allow the chemical production to take advantage of synergies between processes. However, the risks associated with demand uncertainty and supply disruptions or delays may significantly affect tactical decision making of a chemical complex.[4–9] Although inventory improves the service by helping deal with demand uncertainty and providing flexibility, excessive inventory can be costly.[10,11] In addition, a chemical complex usually involves many chemicals, including feedstocks, intermediates, and final products, making it a nontrivial task to determine which chemicals should be stored and what is the optimal inventory level for each of them so as to achieve a certain service level and production target. Thus, cost-effective and agile inventory and production management can provide a competitive advantage for a company in a highly dynamic market.[12,13] Therefore, it is of significant importance to integrate the tactical process planning decisions with the stochastic inventory management decisions across the entire chemical complex, and coordinate the activities of purchase, production, storage, and sale to minimize the total cost. There are several challenges to achieve this goal.

Correspondence concerning this article should be addressed to I. E. Grossmann at grossmann@cmu.edu.
Current Address of Fengqi You: Argonne National Laboratory, Building 240, 9700 South Cass Avenue, Argonne, IL 60439.

The first challenge is how to model the inventory system of a chemical complex, which is more difficult than a multiechelon inventory system and sometimes involves recycle flows. The second one is how to explicitly account for the supply delay and demand uncertainty in the inventory management and production planning. The third challenge is how to integrate the planning of purchases, production, and sales, with inventory control, and how to model the propagation of uncertainties to quantify the internal demand uncertainty of each processes. The last challenge is how to effectively solve the resulting optimization problem that leads to a large-scale nonconvex mixed-integer nonlinear program (MINLP).

In this article, we consider the medium term planning (typically 1–6 months for process companies) of chemical process networks with integration of stochastic inventory management to deal with supply and demand uncertainty. By using the guaranteed service approach[14–17] to model the time delays in the chemical flows, we capture the stochastic nature of the supply and demand uncertainty. An equivalent deterministic optimization model is developed to minimize the total cost including production cost, feedstock purchase cost, cycle inventory, and safety stock costs. The model takes into account multiple tradeoffs and simultaneously determines the optimal purchase amount of each feedstock, production levels in each process, sale amount of each final product and inventory level of each chemical in the chemical process network, and the internal demand of the production processes. The model also captures the risk-pooling effect[18] to allow centralization of safety stock management for chemicals that are consumed/produced in multiple processes. We first formulate the model as an MINLP with a nonconvex objective function and nonconvex constraints. To solve the problem with modest computational times, a tailored branch-and-refine algorithm based on successive piecewise linear approximation is developed for the global optimization. Five examples of chemical complexes with up to 38 processes and 28 chemicals are presented to illustrate the application of the model and the performance of the proposed algorithm.

The outline of this article is as follows. We first review the related literature and the stochastic inventory modeling approach in the next section. The general problem statement is provided after the next section, which is followed by the model formulation for the problem of joint stochastic inventory management and production planning of a chemical process network. In the section of "Illustrative examples," we present the results for three case studies of chemical complexes. To solve the large scale problem, a global optimization algorithm based on successive piecewise linear approximation is presented in the Section "Solution algorithm." The computational results for large-scale instances and the conclusion of this article are then given at the end of this article.

Literature Review

The problem of planning under uncertainty for process network has been extensively studied in the past 20 years, but the inventory issue is usually neglected or coarsely considered without detailed inventory management policy.[6–10,13,19–29] In these models, the safety stock level is given as a parameter and is usually imbedded by including inventory lower bounds of various chemicals or referred to as a "target inventory level" that would lead to some penalty costs if violated. This approach cannot optimize the safety stock levels, especially when considering supply and demand uncertainty. Thus, it can only provide an approximation of the inventory cost, and may lead to suboptimal solutions. Recently, Jung et al.[5] use a simulation–optimization framework to determine the optimal safety stocks levels of a supply chain with consideration of production capacity.

Another body of research closely related to this work is the multiechelon stochastic inventory theory, which can be traced back to the works by Simpson[30] and by Clark and Scarf.[31] There are two major approaches to model the multiechelon inventory system: the stochastic service approach and the guaranteed service approach. For a detailed comparison of these two approaches see Graves and Willems[15] and Humair and Willems.[32] Both approaches have pros and cons: stochastic service approach allows a more exact system understanding that can serve as the building block for more complex systems; the guaranteed service approach models the entire system, which allows a planner to make tactical decisions without the need to approximate portions of the system that are not captured by a simplified topological representation. On the basis of this reason, we choose the guaranteed service approach to model the multiechelon inventory system in this work as we focus on the modeling of inventory allocation across the entire process network. Although the guaranteed service approach has been applied to address diverse problems in multiechelon stochastic inventory management and supply chain optimization,[14,16,33–37] it has not been extended to mid-term planning problems involving inventory systems of chemical complexes that include the production of multiple products in networks with arbitrary topology. Moreover, integrating stochastic inventory management into the tactical planning of process network is nontrivial, and it has not been addressed in the existing literature to the best of our knowledge.

Guaranteed Service Approach for Multistage Stochastic Inventory Systems

In this section, we briefly review some concepts of guaranteed service approach, which is the stochastic inventory model used in this work. Detailed discussions about this approach are given by Graves and Willems[15] and by You and Grossmann.[36]

The main idea of the guaranteed service approach is that the service level for each node in the multiechelon inventory system is fixed, and thus, the optimal inventory level at each node is a function of the worst case replenishment lead time, which is a variable depending on the uncertain demand distribution of this node and the inventory level of its upstream node(s). For example, as shown in Figure 1a, when Node 2 requests a replenishment from its upstream Node 1, the replenishment will arrive after a deterministic processing time P_2, if Node 1 has sufficient inventory to satisfy the demand from Node 2. However, if the inventory level in Node 1 is less than the internal demand from Node 1, this node needs to further wait for the replenishment from its upstream predecessor so as to satisfy the demand from Node

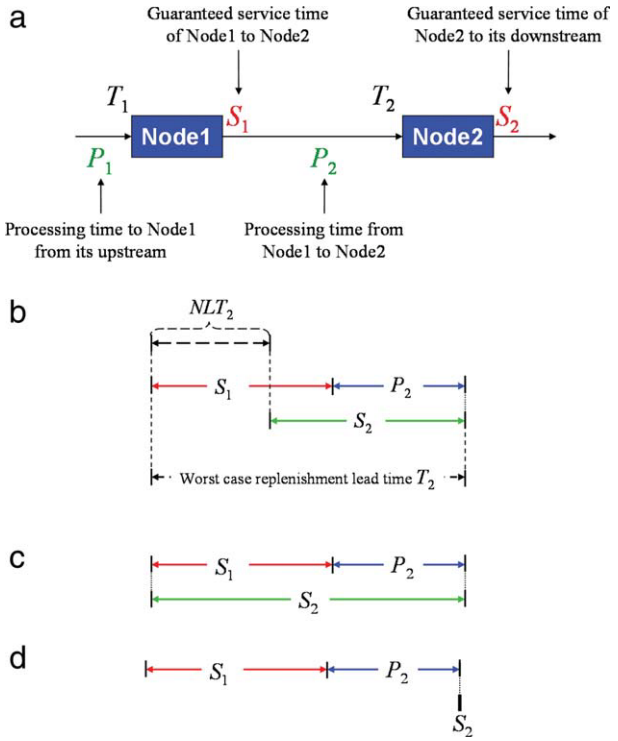

Figure 1. Guaranteed service time, worst case replenishment lead time, and processing time in the guaranteed service approach.

(a) Network precedence of Node 1 and Node 2, (b) timing relationship of Node 2, (c) extreme case when net lead time is zero, this node has zero net lead time and holds zero inventory, i.e., operating as a "pull" system, and (d) extreme case when service time is zero, this node will hold maximum safety stocks and operate as a "push" system. [Color figure can be viewed in the online issue, which is available at wileyonlinelibrary.com.]

2. In this case, it first takes some "waiting time" for the replenishments from the predecessor to arrive at Node 1, and then the deterministic processing time P_2 for the replenishment from Node 1 to arrive at Node 2. Thus, the replenishment lead time of Node 2 is equal to the "waiting time" plus the deterministic processing time. It is important to note that the "waiting time" is not deterministic, but similarly depends on the inventory levels of all the upstream nodes, and thus, it is an uncertain variable. As Node 2 has a fixed service level, the longer is the worst case "waiting time", the more inventories should be hold in Node 2 to deal with the uncertain demand and lead time.

To quantify the "waiting time" for the worst case, guaranteed service approach assumes that each node j in the multi-echelon inventory system guarantees a service time S_j, which is the maximum time that all the demand from its downstream nodes (successor) will be satisfied. Besides, each node j has a net lead time N_j, which is the required time span to cover demand variation with safety stocks at this node. Thus, the timing relationships between the deterministic process time P_j and the times, including the guaranteed service time (GST) S_j, the worst case replenishment lead time T_j, and the net lead time N_j, are given as follows:

(a) The worst case replenishment lead time T_j should be greater than or equal to the summation of the GST of a direct predecessor S_{j-1} and the processing time P_j from the direct predecessor to this node, i.e., $T_j \geq S_{j-1} + P_j$.

(b) The net lead time N_j equals to the difference between the worst case replenishment lead time T_j and the GST to its direct successor S_j, i.e., $N_j = T_j - S_j$.

These timing relationships are shown in Figure 1b. The relationship (a) follows directly from the aforementioned example. The relationship (b) is due to the reason that not all the customer demand of node j at time t must be satisfied immediately, but by the time $t + S_j$. Thus, the safety stocks of node j do not need to cover demand variations over the entire worst case replenishment lead time, but just the difference between the replenishment lead time and the GST to the successors, i.e., the net lead time N_j. The relationships (a) and (b) imply that if the service time of node j equals to the replenishment lead time, i.e., $T_j = S_j$ and $N_j = 0$ as shown in Figure 1c, no safety stock is required in node j because all the downstream demand only needs to be satisfied within the replenishment lead time, i.e., this node is operating in "pull" mode. If the GST S_j is 0, i.e., $N_j = T_j$ as shown in Figure 1d, the node holds the most safety stock because all the demand from the successors are satisfied immediately, i.e., this node is operating in "push" mode.

In the guaranteed service approach, each stage in the inventory system is assumed to operate under a base-stock policy, which is widely used for inventory management across diverse sectors with a common review period.[5,38,39] Furthermore, demand over any time interval is assumed to be normally distributed, e.g., mean μ_j and standard deviation σ_j for the daily demand of node j (if the unit of μ_j is ton/day, the unit of σ_j will be ton/$\sqrt{\text{day}}$). Besides, for node j, there is an associated safety stock factor λ_j, which is given and corresponds to the standard normal deviate of the required service level, i.e., $\Pr(z \leq \lambda_j) = \alpha$ where α is the service level and z is a standard normally distributed random variable with $z \sim N(0,1)$. As the demand rate follows normal distribution, the uncertain demand over the net lead time also follows normal distribution $N(N_j \cdot \mu_j, N_j \cdot \sigma_j^2)$. This yields the safety stock of node j as $\text{SS}_j = \lambda_j \sigma_j \sqrt{N_j}$, and the optimal base-stock level for the inventory position, including the inventory on-hand and inventory in-transit, of this node is given by $\text{BS}_j = N_j \mu_j + \lambda_j \sigma_j \sqrt{N_j}$, which equals to the expected demand over the net lead time plus the safety stock. The base-stock level represents the inventory upper bound, and the lower bound is given by the safety stock level if there is no demand uncertainty. As the physical inventory level is expected to vary between its upper and lower bound if there is no uncertainty (safety stocks are used to hedge uncertain demand), the average on-hand inventory level is given by the safety stock level plus half of the expected demand over the net lead time, i.e., $\text{Inv}_j = N_j \mu_j/2 + \lambda_j \sigma_j \sqrt{N_j}$, where the first term $N_j \mu_j/2$ is the average working inventory (or cycle stock). Note that we neglect pipeline inventory (work-in-process) in the total inventory cost, because the focus of this work is to model the physical storage levels and allocation of chemicals of a chemical complex instead of a supply chain. In addition, the review period has been taken into account as part of the order processing time and considered in the net lead time.

In the guaranteed service approach, the service times from the external suppliers to the inventory system and the service

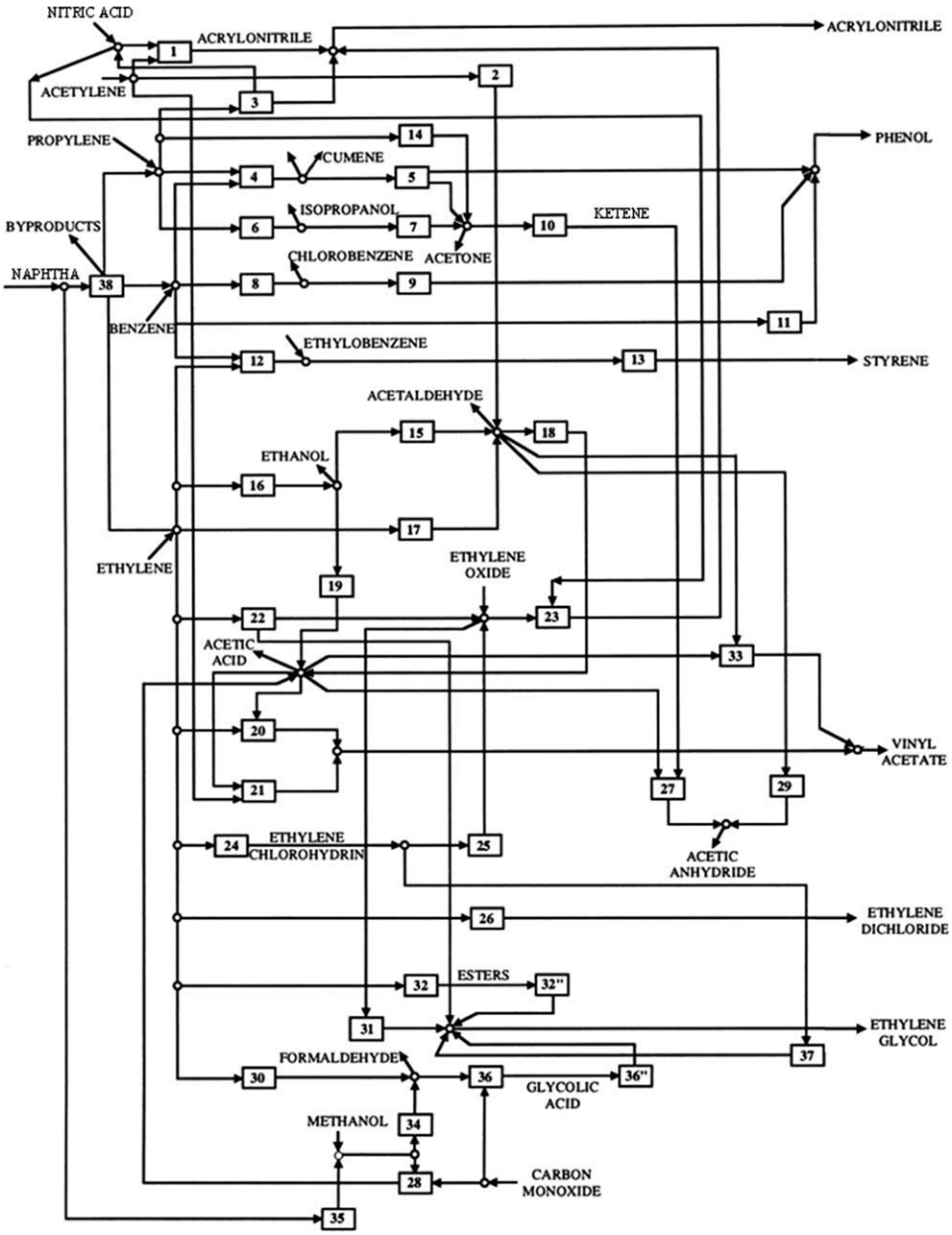

Figure 2. A process network of chemical complex.

times to the external customers are exogenous inputs, which can be treated as parameters in addition to the deterministic processing time P_j and the safety stock factor λ_j. Most of the "virtual" times, including the GST S_j of internal nodes, the worst case replenishment lead time T_j, and the net lead time N_j, are variables to be optimized.

Problem Statement

We are given a process network (Figure 2) consisting of a set of dedicated processes $i \in I$ and a set of chemicals $j \in J$. Each process $i \in I$ has a fixed production capacity Cap_i, a unit production cost δ_i and a production delay (or production time) PD_i. As we consider dedicated processes in this work, the production delays are deterministic parameters that are given. The chemicals could be feedstocks, intermediates, or final products, and each of them can be purchased from the suppliers, produced in the chemical complex and sold to the markets. For each chemical j, there is a unit inventory holding cost h_j and a safety stock factor λ_j, corresponding to the standard normal deviate of the required service level. In every production process i, we are also given a mass balance coefficient η_{ij} for chemical j that is consumed or produced by this process. In addition, the deterministic transfer times from process i that produces chemicals j to the storage tank of this chemical, γ_{ij}, and the deterministic transfer time of chemical j from its storage tank to process i that consumed this chemical, θ_{ij}, are also given and assumed to be deterministic.

The process network also includes a set of suppliers $k \in K$ and a set of markets $l \in L$. For every chemical j, each

supplier k has a supply lower bound a_{jk}^{L} and supply upper bound a_{jk}^{U}, as well as a unit price Γ_{jk}. The GST of chemical j supplied by supplier k, SI_{jk} is also known. The GSTs of suppliers represent the supply uncertainty in terms of service time under the worst case. For every external market l, we are given a normally distributed demand with mean $\overline{\mu}_{jl}$ and standard deviation $\overline{\sigma}_{jl}$ for chemical j, and a required maximum GST SO_{jl}^{U} of each chemical j demanded by this market.

The problem is to simultaneously determine the production level of each process, the working inventory and safety stock levels of each chemical, and the purchase amounts from external suppliers and sale amounts to external markets for each chemical to minimize the total purchase, production, and inventory cost.

Model Formulation

The model will be formulated as an MINLP problem, which will predict the production levels, inventory levels, and purchase and sale amounts of a chemical complex. To explicitly account for the complex interactions between different states of chemicals (feedstocks, intermediate, and final products) and production processes, we use a chemical process network representation, which is given in Figure 3 for the example problem shown in Figure 2. In Figure 3, the numbers inside the boxes indicate processes, and the letters inside the circles are for the chemicals. As a physical interpretation, one could consider these chemical nodes with red circles as the stocking points or storage tanks of chemicals (e.g., see state-task-network[40] model for scheduling). This representation can greatly facilitate the analysis and modeling of the complex interactions between stochastic inventory management and the purchase, production, and sale activities. An MINLP model built based on this network is presented in the following sections. A list of indices, sets, parameters, and variables are given in the Notation.

Stochastic lead time constraints

There is a multiechelon inventory system imbedded in a chemical process network: both chemical nodes and process nodes are stages or echelons of a multiechelon inventory systems, but safety stocks and working inventories (cycle stocks) are only allowed to be maintained in the chemical nodes, i.e., all the processes are operating as a "pull" system with zero net lead time and zero inventory. The inventory model used in this work is based on the guaranteed service approach, in which the service levels of all the stages are known but the lead times are variables. Thus, the inventory model is based on the timing relationships for all the process nodes and chemical nodes in the chemical process network. Thus, we analyze and model the timing relationships, between the deterministic processing time, GSTs, worst case replenishment lead times and net lead times, for all the process nodes and chemical nodes in the chemical process network.

Timing Balance of Process Nodes. The first timing constraint for the process nodes is to define the worst case replenishment lead time. As the production node is treated as a stage in the inventory system with zero inventories, the deterministic processing time should be the time delay of material flow from the "gate" of its direct predecessors to the "gate" of this production node. Thus, the deterministic processing time includes the transfer time from the storage tank to this process and the production delay of this process. It implies that if chemical j is a feedstock of process i, then the worst case replenishment lead time of process $i(TP_i)$ should be greater than or equal to the sum of the GST of chemical j to this process (SC_{ij}), the transfer time (θ_{ij}) from storage tank of chemical j to process i and the production delay of process $i(PD_i)$. This relationship leads to the following inequality.

$$TP_i \geq SC_{ij} + \theta_{ij} + PD_i, \quad \forall j, \quad i \in I(j) \tag{1}$$

where $I(j)$ is the subset of processes that consume chemical j.

Because the production nodes do not hold safety stocks, their net lead times are zero and the GSTs to the successors equal to the worst case replenishment lead time. Thus, if chemical j is a product of process i, the GST of process i to its downstream storage tank for chemical j, SP_{ij}, is equal to the worst case replenishment lead time of process i.

$$SP_{ij} = TP_i, \quad \forall j, \quad i \in O(j) \tag{2}$$

where $O(j)$ is the subset of processes that produce chemical j.

Timing Balance of Chemical Nodes. Using a similar analysis, we can derive the timing constraints for each chemical node. If chemical j, SP_{ij} is a product of process i, the worst case replenishment lead time of chemical j (TC_j) should be greater than the sum of the service time (SP_{ij}) of its direct predecessors, i.e., process i, and the transfer time (γ_{ij}) from process i to storage tank of chemical j.

$$TC_j \geq SP_{ij} + \gamma_{ij}, \quad \forall j, \quad i \in O(j) \tag{3}$$

If chemical j is supplied by external supplier k with nonzero flow rate, the worst case replenishment lead time of chemical j should be greater than the service time of this external supplier, SI_{jk}. This relationship can be modeled by the following constraint,

$$TC_j \geq SI_{jk} \cdot X_{jk}, \quad \forall j, \quad k \in SUP(j) \tag{4}$$

where X_{jk} is a binary variable that is 1 if part or all of the chemical j in the chemical process network is from supplier k, and $SUP(j)$ is the subset of suppliers that can provide chemical j.

If chemical j is a feedstock of process i, the GST of chemical j to its downstream process i (SC_{ij}) should be greater than the difference between the worst case replenishment lead time of chemical j, and the net lead time (N_{ij}) of chemical j for the demand from process i.

$$SC_{ij} \geq TC_j - N_{ij}, \quad \forall j, \quad i \in I(j) \tag{5}$$

If chemical j is sold to external market l, the GST of chemical j to this market, SO_{jl} should be greater than the worst case replenishment lead time of chemical $j-$ the net lead time ($\overline{N}_{jl}$) of chemical j for the demand from market l,

$$SO_{jl} \geq TC_j - \bar{N}_{jl}, \quad \forall j, \quad l \in MKT(j) \tag{6}$$

where $MKT(j)$ is the subset of markets that have positive demand of chemical j.

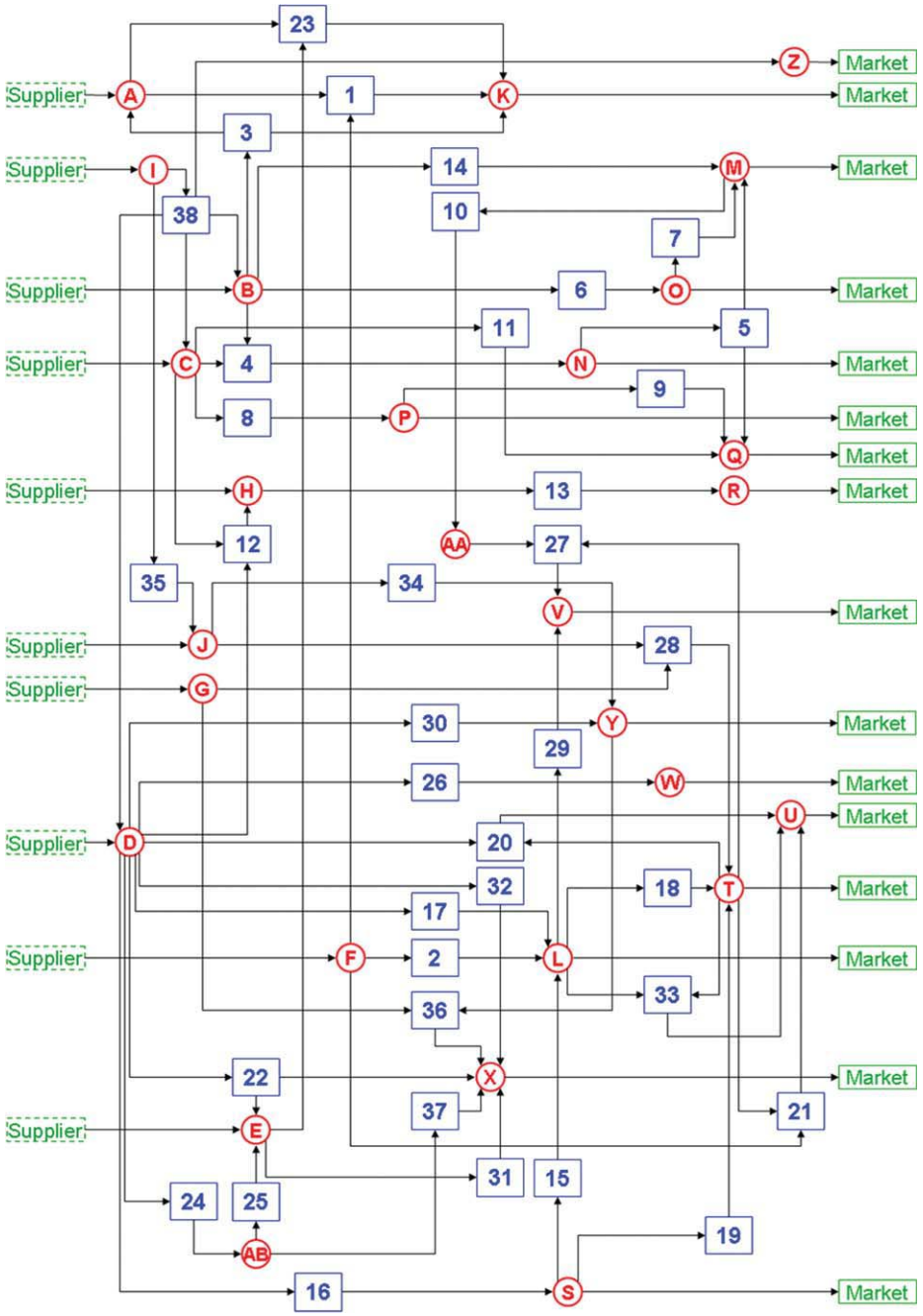

Figure 3. The chemical process network of the example problem shown in Figure 2.

[Color figure can be viewed in the online issue, which is available at wileyonlinelibrary.com.]

In addition, the GST of chemical j to external market l should not exceed its upper bound.

$$\mathrm{SO}_{jl} \leq \mathrm{SO}_{jl}^{\mathrm{U}}, \quad \forall j, \quad l \in \mathrm{MKT}(j) \tag{7}$$

Tactical planning constraints

As we consider the mid-term planning of process networks, the following constraints are introduced to model the production, purchase and sale activities, and account for the mass balance relationships.

Capacity Constraints. The production capacity is measured in terms of the production amount of the main product in each process. Thus, it requires that the production amount (W_{ij}) of main product j in process i does not exceed the capacity, Cap_i.

$$W_{ij} \leq \mathrm{Cap}_i, \quad \forall i, \quad j \in M_i \tag{8}$$

where M_i defines the chemical j that is the main product of process i.

Purchase and Sale Constraint. If supplier k is selected to supply chemical j, the purchase amount (Pu_{jk}) should lie

between their lower and upper bounds; if not, the purchase amount should be zero. This relationship can be modeled by the following constraint.

$$a_{jk}^{\mathrm{L}} \cdot X_{jk} \le \mathrm{Pu}_{jk} \le a_{jk}^{\mathrm{U}} \cdot X_{jk}, \quad \forall j, \quad k \in \mathrm{SUP}(j) \tag{9}$$

Because the unexpected demand is hedged against by safety stocks, the sale amount (Sa_{jl}) of chemical j to market l only needs to satisfy the mean value of the demand, $\overline{\mu}_{jl}$, as in the deterministic process planning. It yields the following constraint.

$$\mathrm{Sa}_{jl} \ge \bar{\mu}_{jl}, \quad \forall j, \quad l \in \mathrm{MKT}(j) \tag{10}$$

Mass Balance Constraints. For chemical j, the total input, including the total external purchase amount and the total production amount, should be equal to the total output, including the total amount consumed by internal processes and the total amount sold to external markets. This mass balance relationship is given by the following constraint.

$$\sum_{k \in \mathrm{SUP}(j)} \mathrm{Pu}_{jk} + \sum_{i \in O(j)} W_{ij} = \sum_{i \in I(j)} W_{ij} + \sum_{l \in \mathrm{MKT}(j)} \mathrm{Sa}_{jl}, \ \forall j \tag{11}$$

where Pu_{jk} is the purchase amount of chemical j from supplier k, and Sa_{jl} is the sale amount of chemical j to market l. Note that inventory is not included in the mass balance constraint (11), because we only consider single time period in this work.

The consumption and production amount (W_{ij}) of chemical j in process i is linearly related to the production amount ($W_{ij'}$) of the main product j' for process i with the mass balance coefficient η_{ij}. This mass balance relationship is given by the following constraint.

$$W_{ij} = \eta_{ij} \cdot W_{ij'}, \quad \forall i, \quad j \in C_i, \quad j' \in M_i \tag{12}$$

where M_i defines the chemical j that is the main product of process i.

Internal demand quantification

In addition to the net lead time, the inventory level of chemical j also depends on the distribution of the uncertain demand. Because the final demand of each chemical in each market is uncertain and follows a normal distribution, the input amount of each feedstock for each process, i.e., the internal demand, is also uncertain. The challenge is that we are only given the mean ($\overline{\mu}_{jl}$) and standard deviation ($\overline{\sigma}_{jl}$) of this chemical's demand in the market l, without knowing the detailed distribution of the "internal" demands.

Probability Distribution of Internal Demands. As the final demand at each market follows a normal distribution, it follows that the internal demands are also normally distributed due to the linear mass balance constraint (11), to Cramér's theory (if the sum of some independent real-valued random variables is a normal random variable, then both all these random variables must be normally distributed as well), and to the perfect splitting property of the Gaussian distribution (the sum/difference of independent normal random variables also follows normal distribution with a mean as the sum/difference of the means of those random variables and a variance as the sum/difference of those variances). As the mass balance constraints (11) require that the net input of each chemical should be equal to the net output, and the sale constraint (10) considers production targets as the mean values of market demands, the consumption amount of the feedstock j in process i (W_{ij}) corresponds to the mean value of the associated internal demand.

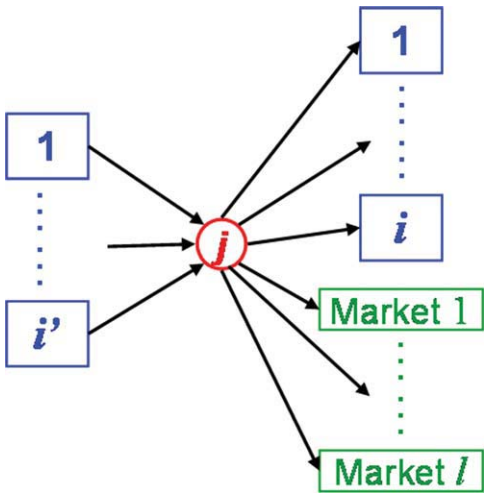

Figure 4. Input and output relationship of a chemical node in the PCN.

[Color figure can be viewed in the online issue, which is available at wileyonlinelibrary.com.]

To determine the variance of an internal demand, let us first consider their variance-to-mean (VTM) ratios. The VTM ratio is unchanged when a normal distribution is randomly split into a few distributions, i.e., there is a linear relationship between the variance and mean. For process i, if the demands of its products increase, its consumption amounts of feedstocks should also increase. Thus, to ensure a continuous and stable production of the process, and to hedge against the uncertain demand, the VTM ratios for all internal demands of its feedstocks, denoted as RP_i, should be the same. As we know that the mean value of the internal demand of chemical j in process i, $i \in I(j)$ is W_{ij}, which is the consumption amount of feedstock j in this process, the variance (V_{ij}) of the internal demand of chemical j in process i is then given by the following constraint.

$$V_{ij} = \mathrm{RP}_i \cdot W_{ij}, \quad \forall j, \quad i \in I(j) \tag{13}$$

Uncertainty Propagation Through the Chemical Process Network. Because the information flow transfers from downstream to upstream, i.e., from the markets to the suppliers, we can use a "backward" derivation to determine the VTM ratios of the internal demands.

Let us first consider the input and output relationship of a chemical node as shown in Figure 4. The successors of chemical node j may include process i, $i \in I(j)$ which has normally distributed demand of chemical j with variance V_{ij} and VTM ratio RP_i, and market l, $l \in \mathrm{MKT}(j)$, which also has normally distribution demand of chemical j with variance $\overline{V}_{jl}$, i.e., $\overline{V}_{jl} = \overline{\sigma}_{jl}^2$, and VTM ratio $\overline{R}_{jl}$, i.e., $\overline{R}_{jl} = \overline{\sigma}_{jl}^2/\overline{\mu}_{jl} = \overline{V}_{jl}/\overline{\mu}_{jl}$. Thus, the total demand of chemical j from the markets and downstream

processes also follows a normal distribution with a mean given by $(\sum_{i\in I(j)} W_{ij} + \sum_{l\in \mathrm{MKT}(j)} \mathrm{Sa}_{jl})$ and a variance given by $(\sum_{i\in I(j)} V_{ij} + \sum_{l\in \mathrm{MKT}(j)} \bar{R}_{jl}\cdot \mathrm{Sa}_{jl})$. Hence, the VTM ratio of the demand of chemical j is given by $(\sum_{i\in I(j)} V_{ij} + \sum_{l\in \mathrm{MKT}(j)} \bar{R}_{jl}\cdot \mathrm{Sa}_{jl})/(\sum_{i\in I(j)} W_{ij} + \sum_{l\in \mathrm{MKT}(j)} \mathrm{Sa}_{jl})$. If we denote RC_j as the VTM ratio of the demand of product j in process i, $i \in O(j)$, then the value of RC_j is determined by modeling the uncertainty propagation from the downstream to upstream through the chemical node. There are two potential cases for uncertainty propagation: the ideal case and the worst case.

In the ideal case, RC_j equals to the VTM ratio of the total demand of chemical j from markets and downstream processes, i.e., $(\sum_{i\in I(j)} V_{ij} + \sum_{l\in \mathrm{MKT}(j)} \bar{R}_{jl}\cdot \mathrm{Sa}_{jl})/(\sum_{i\in I(j)} W_{ij} + \sum_{l\in \mathrm{MKT}(j)} \mathrm{Sa}_{jl})$. One can draw an analogy of this "ideal" uncertainty propagation to the "pooling" problem[41] with flow rate similar to the total demand rate and the concentration similar to the VTM ratio, although in this case, we model the information flow transfers from downstream to upstream. Thus, the uncertainty propagation through a chemical node in the ideal case can be modeled with the following constraint.

$$\mathrm{RC}_j \cdot \left(\sum_{i\in I(j)} W_{ij} + \sum_{l\in \mathrm{MKT}(j)} \mathrm{Sa}_{jl}\right) = \sum_{i\in I(j)} V_{ij} + \sum_{l\in \mathrm{MKT}(j)} \bar{R}_{jl}\cdot \mathrm{Sa}_{jl}, \quad \forall j \quad (14)$$

where the right hand side of this constraint involves the product of two variables, i.e., bilinear terms.

With constraint (14), we can see that the uncertainty propagation under the ideal case maintains the conservation of variance. However, in most cases, the level of uncertainty amplifies as the information flow transfers from downstream to upstream, i.e., the "bullwhip effect."[42] Thus, we address this issue by considering another type of uncertainty propagation—the "worst" case propagation.

In the worst case, the "outbound" information stream from a chemical node to one of its direct predecessors (note that information transfers from downstream to upstream) should have a VTM ratio equal to the maximum VTM ratios of all the "inbound" information stream of this chemical node. In other words, the VTM ratio (RC_j) of the demand of product j of process i, $i \in O(j)$, equals to the maximum VTM ratio of chemical j in the downstream processes i, $i \in I(j)$, and markets l, $l \in \mathrm{MKT}(j)$, i.e., $\mathrm{RC}_j = \max\{\max_{i\in I(j)}\{\mathrm{RP}_i\}, \max_{l\in \mathrm{MKT}(j)}\{\bar{R}_{jl}\}\}$. This relationship can be modeled by the following two constraints.

$$\mathrm{RC}_j \geq \mathrm{RP}_i, \quad \forall j, \quad i \in I(j) \quad (15)$$

$$\mathrm{RC}_j \geq \bar{R}_{jl}, \quad \forall j, \quad l \in \mathrm{MKT}(j) \quad (16)$$

The differences and similarities of these two approaches will be illustrated in examples 1–3. In general, the worst case approach is relatively conservative and may lead to higher inventories and service levels than the ideal case approach. From the modeling perspective, constraint (14) includes nonconvex and nonlinear bilinear terms on the left hand side, whereas constraint (15) and (16) are simply linear constraints. Although there is no clear rule how the uncertainty propagates through a chemical process network from the markets to the suppliers, the ideal case approach and the worst case approach represent two extreme scenarios. As the inventory has to deal with unexpected situations and accounts for the worst case, the "worst" case uncertainty propagation might be a more suitable approach. A detailed comparison of these two approaches will be presented in Example 3.

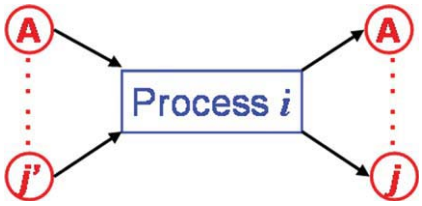

Figure 5. Input and output relationship of a process node in the PCN.

[Color figure can be viewed in the online issue, which is available at wileyonlinelibrary.com.]

In addition to the above constraints, we also need to consider how the VTM ratios change as the information flow transfers through a process node. The successors of a process node i are all chemical nodes, as shown in Figure 5, and all these chemical nodes are the products of this process. Because the process operates in the "pull" mode and all the products are produced simultaneously with a linear mass balance relationship as in constraint (12), the VTM ratio for all demands of its feedstocks, RP_i, should be greater than or equal to the corresponding ratio of any of its products. Thus, we have the following constraint to model this relationship.

$$\mathrm{RP}_i \geq \mathrm{RC}_j, \quad \forall j, \quad i \in O(j) \quad (17)$$

Non-negative constraints

All continuous variables must be nonnegative and the binary variables should be 0 or 1.

$$\mathrm{SC}_{ij} \geq 0, \quad N_{ij} \geq 0, \quad V_{ij} \geq 0, \quad \forall j, \quad i \in I(j) \quad (18.1)$$

$$\mathrm{SP}_{ij} \geq 0, \quad \forall j, \quad i \in O(j) \quad (18.2)$$

$$W_{ij} \geq 0, \quad \forall j \in C_i \quad (18.3)$$

$$\mathrm{RP}_i \geq 0, \quad \mathrm{TP}_i \geq 0, \quad \forall i \quad (18.4)$$

$$\mathrm{RC}_j \geq 0, \quad \mathrm{TC_j} \geq 0, \quad \forall \mathrm{j} \quad (18.5)$$

$$\mathrm{Pu}_{jk} \geq 0, \quad \forall j, \quad k \in \mathrm{SUP}(j) \quad (18.6)$$

$$\mathrm{Sa}_{jl} \geq 0, \quad \mathrm{SO}_{jl} \geq 0, \quad \bar{N}_{jl} \geq 0, \quad \forall j, \quad l \in \mathrm{MKT}(j) \quad (18.7)$$

$$X_{jk} \in \{0,1\}, \quad \forall j, \quad k \in \mathrm{SUP}(j) \quad (18.8)$$

Objective function

The objective of this problem is to minimize the total cost, including feedstock purchase cost, production cost, and inventory cost.

The purchase cost is given by the summation of products of the unit price of chemical and the total purchase amount, $\sum_k \sum_{j\in \mathrm{SUP}(k)} \Gamma_{jk} \cdot \mathrm{Pu}_{jk}$, where Γ_{jk} is the unit purchase price of chemical j from supplier k.

The production cost is given by the summation of products of the unit processing cost and the production amount of main product, $\sum_i \sum_{j\in M_i} \delta_i \cdot W_{ij}$, where δ_i is the unit production cost of process i.

The inventory cost includes cycle stock cost and safety stock cost. As the net lead time of chemical j for the uncertain demand from downstream process i and external market are N_{ji} and $\overline{N}_j$, respectively, the uncertain internal and external demand of chemical j follows normal distribution with mean $(\sum_{l\in \mathrm{MKT}(j)} \bar{N}_{jl} \cdot \bar{\mu}_{jl} + \sum_{i\in I(j)} N_{ij} \cdot W_{ij})$ and variance $(\sum_{l\in \mathrm{MKT}(j)} \bar{N}_{jl} \cdot \bar{V}_{jl} + \sum_{i\in I(j)} N_{ij} \cdot V_{ij})$. Thus, the optimal cycle stock of chemical j is given by $(\sum_{l\in \mathrm{MKT}(j)} \bar{N}_{jl} \cdot \bar{\mu}_{jl} + \sum_{i\in I(j)} N_{ij} \cdot W_{ij})/2$, and the safety stocks of chemical j is given by $\lambda_j \sqrt{\sum_{l\in \mathrm{MKT}(j)} \bar{N}_{jl} \cdot \bar{V}_{jl} + \sum_{i\in I(j)} N_{ij} \cdot V_{ij}}$, where λ_j is the safety stock factor of chemical j. Note that this approach is consistent with the "risk-pooling" effect,[18] where we centralize the inventory management of chemical j and aggregate all the downstream demands into the chemical node. As will be shown in Example 2, this centralized approach will lead to potential reduction of total cost when compared with the decentralized inventory management, i.e., maintain the inventory in each individual process of a chemical complex.

With the aforementioned cost components, the objective function for minimizing the total cost is given in (19).

$$\begin{aligned}\min \quad & \sum_i \sum_{j\in M_i} \delta_i \cdot W_{ij} + \sum_k \sum_{j\in \mathrm{SUP}(k)} \Gamma_{jk} \cdot \mathrm{Pu}_{jk} \\ & + \sum_j \frac{h_j}{2} \cdot \left(\sum_{l\in \mathrm{MKT}(j)} \bar{N}_{jl} \cdot \bar{\mu}_{jl} + \sum_{i\in I(j)} N_{ij} \cdot W_{ij} \right) \\ & + \sum_j \left(h_j \cdot \lambda_j \sqrt{\sum_{l\in \mathrm{MKT}(j)} \bar{N}_{jl} \cdot \bar{V}_{jl} + \sum_{i\in I(j)} N_{ij} \cdot V_{ij}} \right) \end{aligned} \tag{19}$$

where h_j is the unit inventory holding cost of chemical j.

Nonconvex MINLP model

The constraints and objective function discussed above yield two MINLP models, one is for the "ideal" case uncertainty propagation, denoted as model (P1), and the other is for the "worst" case uncertainty propagation, denoted as model (P2). The model for ideal case includes constraints (1)–(14), (17), (18), and the objective function (19). The model for worst case includes constraints (1)–(13), (15)–(18), and the objective function (19). Both models are nonconvex, because constraints (13) and (14) include bilinear terms, and the objective function (19) has both square root terms and bilinear terms.

Illustrative Example

To illustrate the application of the MINLP models (P1) and (P2), we first consider three small-scale examples.

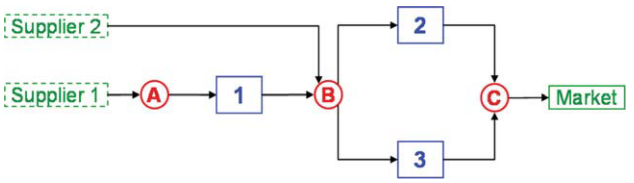

Figure 6. Example 1 with three chemicals, three processes, two suppliers, and one market.

[Color figure can be viewed in the online issue, which is available at wileyonlinelibrary.com.]

Example 1: Timing relationship and mass balance

The first example is for a chemical process network with three chemicals, three processes, two suppliers, and one market, taken from Sahinidis and Grossmann.[3] The chemical process network of this problem is given in Figure 6.

In this problem, the safety stock factor λ_j for all the chemicals are the same and equal to 2.0537, corresponding to a 98% service level, i.e., $\Pr(z \le 2.0537) = 98\%$ for $z \sim N(0,1)$. The demand of Chemical C in the market follows a normal distribution with a mean of 100 ton/day and a standard deviation of 20 ton/$\sqrt{}$day. The maximum GST of Chemical C to the market is fixed to zero. The deterministic transfer times from process i to storage tank of chemical j (γ_{ij}) and from storage tank of chemical j to process i (θ_{ij}) are neglected and set to zero. The remaining input data are given in Table 1.

The MINLP model (P1) for "ideal case" uncertainty propagation involves two binary variables, 36 continuous variables, and 38 constraints, and the MINLP model (P2) for "worst case" uncertainty propagation involves two binary variables, 36 continuous variables, and 39 constraints. As the problem sizes are rather small, we globally optimize both instances using the BARON solver[43] with GAMS,[44] and both CPU times are less than 1 s for obtaining optimal solutions with 0% optimality margin.

Both instances lead to the same optimal solution, and a minimum daily total cost of \$22,007.07/day. The reason is that this problem involves only one market, which only has demand of Chemical C. Thus, all the VTM ratios in this chemical process network equal to the VTM ratio of this final demand, no matter how we consider the uncertainty propagation. Note that in general cases, the "worst case" model (P2) may predict larger variances of internal demands, and consequently larger optimal safety stocks and higher total cost, compared with the "ideal case" model (P1).

The optimal solutions are shown in Table 2 and Figure 7. We can see that the daily total safety stock cost of this chemical complex is \$1165.4/day, which is around 5.3% of the daily total cost, and the total cost of cycle stocks is \$3166.4/day, which is around 14.4% of the daily total cost. The total purchase cost and total production cost represent 27.2% and 53.2% of the daily total cost, respectively. The production levels are given in Figure 7a. We can see that Process 1 and Process 3 are operating at full capacity. For Process 1, the unit cost of Chemical B, including the unit production cost of Process 1 (\$50/ton) and the purchase cost of 1.11 tons of Chemical A from Supplier 1 (\$44.4/ton of Chemical B), is less than the purchase cost of Chemical from Supplier 2 (\$152/ton). For Process 3, although its unit production cost is higher than the one of Process 2, it

Table 1. Input Data of Example 1

	Process 1	Process 2	Process 3
Main product	Chemical B	Chemical C	Chemical C
Production capacity Cap_i (ton/day)	100	80	70
Unit production cost δ_i (\$/ton)	50	60	70
Production delay PD_i (day)	2	3	2
	Chemical A	Chemical B	Chemical C
Unit inventory cost h_j (\$/ton/day)	1.5	4.5	9.0
	η_{ij}: mass balance coefficients (positive for inputs and negative for outputs)		
	Chemical A	Chemical B	Chemical C
Process 1	1.11	−1	
Process 2		1.22	−1
Process 3		1.05	−1
	Γ_{jk}: unit purchase cost (\$/ton)		
	Chemical A	Chemical B	Chemical C
Supplier 1	40		
Supplier 2		152	
	SI_{jk}: guaranteed service time (day)		
	Chemical A	Chemical B	Chemical C
Supplier 1	3		
Supplier 2		8	
	a_{jk}^{U}: upper bound of availability (ton/day)		
	Chemical A	Chemical B	Chemical C
Supplier 1	200		
Supplier 2		100	

requires less Chemical B as feedstock for the product of Chemical C, and consequently less unit cost of the final product. The purchase and sale activities are then coordinated based on the production level to ensure the mass balance in each process, supplier, and market.

The detailed optimal net lead times and GSTs of all the nodes in this chemical process network are given in Figure 7b. The optimal solution shows that the chemical process network needs to hold inventory for the feedstock Chemical A, intermediate Chemical B, and the final product Chemical C. The reason is that the GST of supplier 1 plus the production delay of Process 1 is 5 days, but the GST of supplier 2 is 8 days. This implies that no matter how much inventory we hold for Chemical A, the worst case replenishment lead time for Chemical B is always 8 days. Thus, an economic way is to hold zero inventory of Chemical A, i.e., operating as ''pull'' system with zero net lead time, and quote a GST of 3 days to Process 1. Now, consider the timing relationship between Chemicals B and C and Process 2 and Process 3. Because the unit inventory cost of Chemical B (\$4.5/day/ton) is less the one for Chemical C (\$9/day/ton), it is optimal to hold as much inventory of Chemical B as possible, so as to reduce the required stock level of Chemical C. Thus, Chemical B quotes a GST of 0 day to Process 2 and allows its net lead time to Process 2 equal to its worst case replenishment lead time, 8 days. However, Chemical B guarantees a service time of 1 day to Process 3, and has the corresponding net lead time as 7 days, instead of the maximum of 8 days. This is due to the difference between the production delays of Process 2 (3 days) and Process 3 (2 days). As Chemical 3 needs to have zero GST to the market and holds inventories for a net lead time of 3 days, i.e., ''push'' system, it is optimal to have the production delay of Process 3 plus the GST to this process equal to 3 days as well. These results show that inventory allocation of the chemical process network leads to a hybrid ''push–pull'' system, where each node either does not hold inventory or holds maximum required inventory. What we observed in this example is consistent and similar to the phenomena discovered by Simpson[30] for multistage ''serial'' inventory system. It is also interesting to note that all the optimal GSTs and net

Table 2. Optimal Solution of Example 1

	Chemical A	Chemical B	Chemical C
Total safety stock (ton)	0	116.70	71.14
Total cycle stock (ton)	0	403.65	150
Total safety stock cost ($/day)	0	525.3	640.3
Total cycle stock cost ($/day)	0	1816.4	1350
	W_{ij}: production/consumption amount (ton/day)		
Process 1	111	100	
Process 2		36.6	30
Process 3		73.5	70
	V_{ij}: variance of internal demand (ton^2/day)		
Process 1	444		
Process 2		146.4	
Process 3		294	
	Pu_{jk}: purchase amount (ton/day)		
Supplier 1	111		
Supplier 2		10	
	Sa_{jl}: sale amount (ton/day)		
Market			100

lead times happen to be integer, although we do not restrict them to be integer values.

Example 2: Risk pooling effect

The second example is for a chemical process network with 10 chemicals, six processes, two suppliers and one market, taken from Iyer and Grossmann[45] and shown in Figure 8a. In this problem, the safety stock factor for all the chemicals are also set to 2.0537, corresponding to 98% service level. The maximum GST of all the chemicals to the market are zero, and the purchase lower bounds are all set to zero, too. The deterministic transfer times from process i to storage tank of chemical j (γ_{ij}) and from storage tank of chemical j to process i (θ_{ij}) are neglected. All the external demands of chemicals in the market follow normal distributions. There are two suppliers: an international one (Supplier 1) and a domestic one (Supplier 2). In general, the international supplier has higher GSTs to supply the feedstocks, but lower unit purchase costs. The detailed input data are given in Table 3.

In this example, we consider two instances, the centralized inventory management and the decentralized inventory management. The difference between them is that the centralized one takes into account the "risk pooling" effect[18] in the inventory model, as in model (P1) and (P2), whereas the decentralized one does not group the inventories of the chemicals, but use a simple "rule of thumb" to maintain the individual storages for the feedstocks and/or products of all the processes and markets, i.e., each process manages its own inventories without coordination throughout the chemical complex. The chemical process networks of these two instances are given in Figures 8a, b, respectively, and the chemicals in these two chemical process networks are listed in Table 4. When compared with the centralized inventory management instance, the "decentralized" one has more chemical nodes due to the disaggregation of some chemicals as feedstocks and products of process.

We first solved the instance for centralized inventory management with models (P1) and (P2) using GAMS/BARON, because there are only eight binary variables, 108 continuous variables, and 124 constraints in (P1) and eight binary variables, 108 continuous variables, and 128 constraints in (P2). The CPU times are both less than 1 s, and both models lead to the same global optimal solution with a minimum daily total cost of $312,288.81/day. The reason is that all the VTM ratios of internal demands in the chemical process networks are the same in both optimal solutions, except those for the feedstocks of Process 4, Chemicals B and C. However, the optimal net lead times of Chemical B to Process 4 and of Chemical C to Process 4 are zero in both optimal solutions. This implies that no safety stocks are held for the feedstocks of Process 4. Therefore, the differences between the two approaches for uncertainty propagation are not reflected in the total minimum cost.

The optimal inventory levels and production, purchase and sale levels are shown in Table 5. The optimal total daily safety stock cost is $5296.6/day, which is around 1.7% of the daily total cost, and the total cost of cycle stocks is $13,390.4/day, which is around 4.3% of the daily total cost. The total purchase cost and total production cost represent 81% and 13% of the daily total cost, respectively. Thus, the total inventory cost is almost half of the production cost, despite the high-feedstock cost. In terms of the production levels, we can see from Table 5 that all the processes are operating with around 80% capacity due to the relatively low

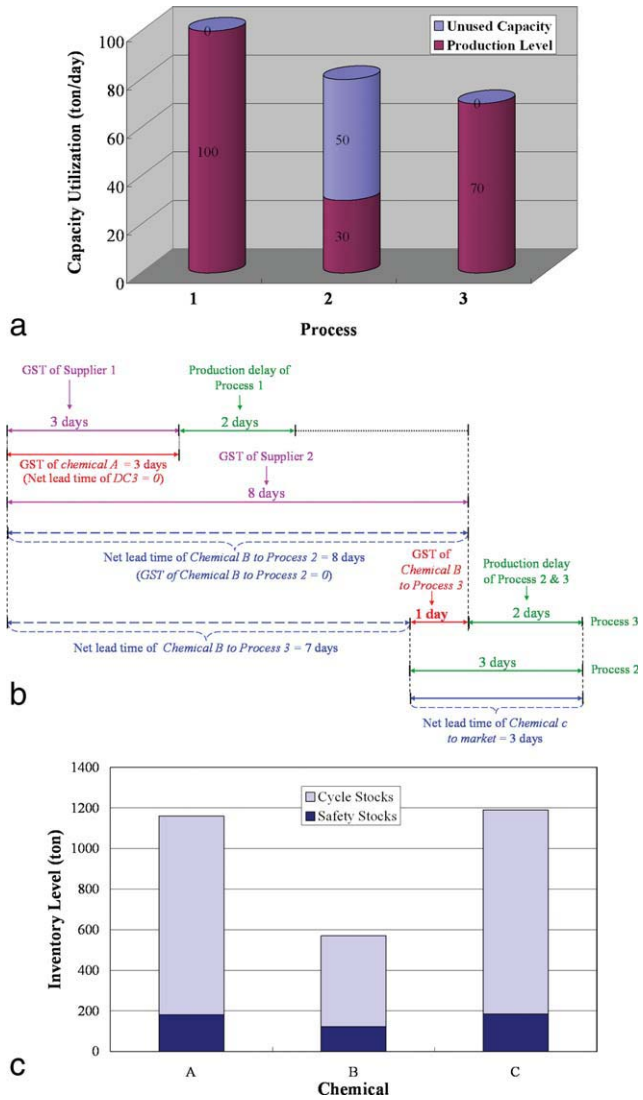

Figure 7. Optimal solution of Example 1 with three chemicals, three processes, two suppliers, and one market.

(a) Optimal production levels and unused capacities of each process for Example 1, (b) timing relationship for the optimal solution of Example 1, and (c) optimal inventory levels of Example 1. [Color figure can be viewed in the online issue, which is available at wileyonlinelibrary.com.]

demand. We can also see that all the purchases of acetylene are from the internal supplier (Supplier 1) due to the relatively low price ($550/ton vs. $600/ton). However, all the purchases of propylene are from the domestic supplier (Supplier 2), because the long lead time of the international supplier leads to higher inventory costs, which offsets its price advantage ($400/ton vs. $405/ton). The results reveal the trade-offs between process planning and inventory management. It is interesting to note that due to the co-production of phenol and acetone in Process 5, the sale amount of acetone is higher than the production target.

In the second instance of this problem, we consider the decentralized inventory management, of which the chemical process network is given in Figure 8b. The models for the decentralized inventory management instance are almost the same as (P1) and (P2), except the safety stock cost term in the objective function. Recall that for chemical j, its uncertain demand from downstream process i has a variance of V_{ij} and a net lead time of N_{ji}, and its uncertain demand from downstream market l (if applicable) has a variance of $\overline{V}_{jl}$ and a net lead time of $\overline{N}_j$. Thus, in the decentralized inventory management case, the optimal safety stocks of chemical j for downstream process i is $\lambda_j\sqrt{N_{ij}\cdot V_{ij}}$, and for market l is $\lambda_j\sqrt{\bar{N}_{jl}\cdot\bar{V}_{jl}}$. Therefore, the total safety stock of chemical j under the decentralized inventory management mode is $\lambda_j\left(\sum_{l\in\mathrm{MKT}(j)}\sqrt{\bar{N}_{jl}\cdot\bar{V}_{jl}}+\sum_{i\in I(j)}\sqrt{N_{ij}\cdot V_{ij}}\right)$. Using a similar approach, it is easy to prove that the optimal cycle stocks of chemical j is the same in both instances, and is given by $\left(\sum_{l\in\mathrm{MKT}(j)}\bar{N}_{jl}\cdot\bar{\mu}_{jl}+\sum_{i\in I(j)}N_{ij}\cdot W_{ij}\right)/2$. Therefore, the models for the decentralized inventory management have the same constraints as (P1) and (P2), but a new objective function is given in (20).

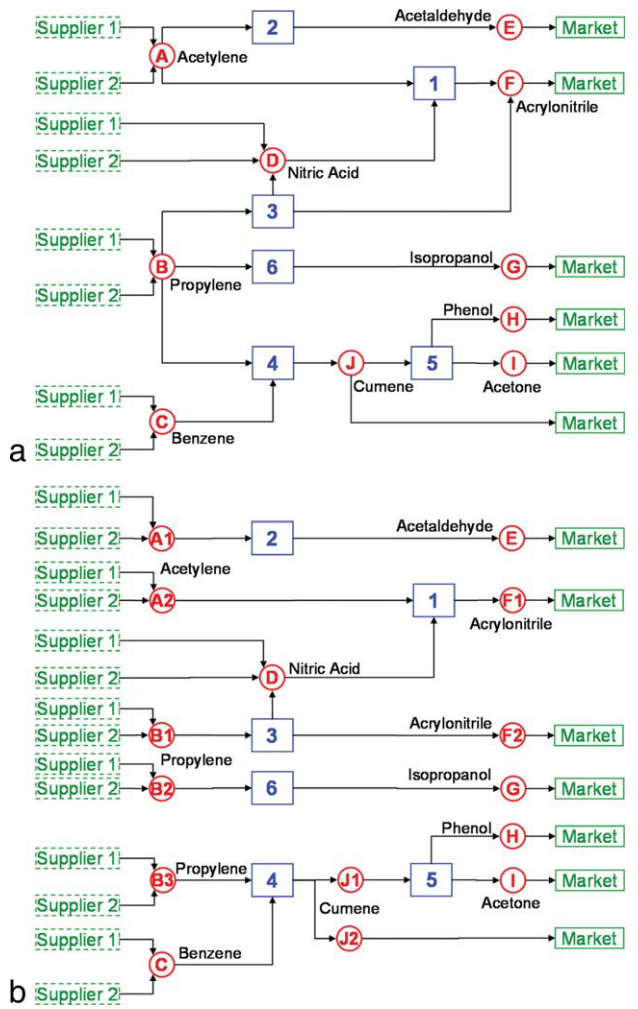

Figure 8. Example 2 with 10 chemicals, six processes, two suppliers, and one market.

(a) Chemical process network of Example 2, centralized inventory management. (b) Chemical process network of Example 2, "decentralized" inventory management. [Color figure can be viewed in the online issue, which is available at wileyonlinelibrary.com.]

Table 3. Input Data of Example 2

	Production capacity Cap_i (ton/day)		
Process 1	180	Process 4	400
Process 2	100	Process 5	200
Process 3	50	Process 6	100
	Unit production cost δ_i ($/ton)		
Process 1	55	Process 4	50
Process 2	60	Process 5	50
Process 3	70	Process 6	90
	Production delay PD_i (day)		
Process 1	2	Process 4	4
Process 2	3	Process 5	5
Process 3	2	Process 6	4
	Unit inventory cost h_j ($/ton/day)		
Acetylene	1.5	Acrylonitrile	8
Propylene	2.5	Isopropanol	5
Benzene	5.0	Phenol	3
Nitric acid	5.0	Acetone	7
Acetaldehyde	10	Cumene	2
	Mass balance relationship		
Process 1	0.63 Acetylene + 0.58 nitric acid → acrylonitrile		
Process 2	0.64 Acetylene → 0.55 nitric acid + acetaldehyde		
Process 3	1.25 Propylene → 0.9 nitric acid + acrylonitrile		
Process 4	0.4 Propylene + 0.69 benzene → cumene		
Process 5	2.3 Cumene → 1.7 phenol + acetone		
Process 6	0.74 Propylene → isopropanol		
	$\bar{\mu}_{jl}$: mean value of external demands (ton/day)		
Acetaldehyde	80	Phenol	200
Acrylonitrile	110	Acetone	100
Isopropanol	70	Cumene	70
	$\bar{\sigma}_{jl}$: standard deviation of external demands (ton/$\sqrt{\text{day}}$)		
Acetaldehyde	20	Phenol	50
Acrylonitrile	30	Acetone	30
Isopropanol	20	Cumene	20

	Γ_{jk}: unit purchase cost ($/ton)			
	Acetylene	Propylene	Benzene	Nitric acid
Supplier 1	550	400	440	820
Supplier 2	600	405	445	820
	SI_{jk}: guaranteed service time (day)			
	Acetylene	Propylene	Benzene	Nitric acid
Supplier 1	14	13	13	19
Supplier 2	2	3	2	4
	a_{jk}^{U}: upper bound of availability (ton/day)			
	Acetylene	Propylene	Benzene	Nitric acid
Supplier 1	100	200	200	50
Supplier 2	50	250	100	100

Table 4. List of Chemicals in Example 2

A	Acetylene	F	Acrylonitrile
B	Propylene	G	Isopropanol
C	Benzene	H	Phenol
D	Nitric acid	I	Acetone
E	Acetaldehyde	J	Cumene

$$\min \quad \sum_i \sum_{j\in M_i} \delta_i \cdot W_{ij} + \sum_k \sum_{j\in \mathrm{SUP}(k)} \Gamma_{jk} \cdot \mathrm{Pu}_{jk} + \sum_j \frac{h_j}{2} \cdot \left(\sum_{l\in \mathrm{MKT}(j)} \bar{N}_{jl} \cdot \bar{\mu}_{jl} + \sum_{i\in I(j)} N_{ij} \cdot W_{ij} \right) + \sum_j \left[h_j \cdot \lambda_j \left(\sum_{l\in \mathrm{MKT}(j)} \sqrt{\bar{N}_{jl} \cdot \bar{V}_{jl}} + \sum_{i\in I(j)} \sqrt{N_{ij} \cdot V_{ij}} \right) \right] \quad (20)$$

We again use GAMS/BARON to solve the new models, which have the same variables and constraints as (P1) and (P2), respectively. Similarly to the previous instance, the ideal case and the worst case uncertainty propagation both lead to the same global minimum cost, $ 312,785.15/day, of which $5792.9/day is safety stock cost, $13,390.4/day is the cycle stock cost, $40,708.4/day is the production cost, and

Table 5. Optimal Solution of the "Centralized" Inventory Management Instance in Example 2

	Production amount in terms of main product W_{ij_m} (ton/day)			
Process 1	66.89	Process 4	340.59	
Process 2	80	Process 5	117.65	
Process 3	43.11	Process 6	70	
	Total safety stock (ton)			
Acetylene	188.35	Acrylonitrile	87.13	
Propylene	96.56	Isopropanol	82.15	
Benzene	0	Phenol	229.61	
Nitric acid	51.746	Acetone	137.77	
Acetaldehyde	71.142	Cumene	520.77	
	Total cycle stock (ton)			
Acetylene	653.39	Acrylonitrile	110	
Propylene	158.53	Isopropanol	140	
Benzene	0	Phenol	500	
Nitric acid	38.80	Acetone	250	
Acetaldehyde	120	Cumene	2895	

	Pu_{jk}: purchase amount (ton/day)		
	Acetylene	Propylene	Benzene
Supplier 1	93.34	0	200
Supplier 2	0	241.92	35.01

	Sa_{jl}: sale amount to the market (ton/day)		
Acetaldehyde	80	Phenol	200
Acrylonitrile	110	Acetone	117.647
Isopropanol	70	Cumene	70

Table 6. Optimal Solution of the "Decentralized" Inventory Management Instance in Example 2

	Total safety stock (ton)		
Acetylene	265.63	Acrylonitrile	87.13
Propylene	135.89	Isopropanol	82.15
Benzene	0	Phenol	229.61
Nitric acid	51.75	Acetone	137.77
Acetaldehyde	71.14	Cumene	661.81
	Total cycle stock (ton)		
Acetylene	653.39	Acrylonitrile	110
Propylene	158.53	Isopropanol	140
Benzene	0	Phenol	500
Nitric acid	38.80	Acetone	250
Acetaldehyde	120	Cumene	2895

$252,893.4/day is the purchase cost. The new models predict exactly the same optimal production, purchase and sales levels, and costs as in the previous instance, but higher inventory levels. The optimal inventory levels of chemicals are listed in Table 6, and a comparison between the optimal safety stocks of the centralized and decentralized inventory management are presented in Figure 9, which shows that the safety stocks of acetylene, propylene, and cumene have been significantly reduced by using centralized inventory management to account for "risk pooling," and in turn suggests the applicability of the proposed models.

Example 3: Recycle and uncertainty propagation

In the third example, we consider a chemical process network with seven chemicals, eight processes, two suppliers, and one market. The chemical process network of this problem is given in Figure 10. In this example, we still consider 98% service level for all the chemicals. The demands of Chemicals D and G in the market follow a normal distribution with mean values of 120 ton/day and 90 ton/day, and standard deviation of 40 ton/$\sqrt{}$day, 50 ton/$\sqrt{}$day, respectively. The purchase lower bounds, the maximum GSTs of chemicals to the market, and the deterministic transfer times from process i to storage tank of chemical j (γ_{ij}) and from storage tank of chemical j to process i (θ_{ij}) are all set to zero. The remaining input data are given in Table 7.

From Figure 10, we can see that the chemical process network of this example is different from the previous ones—there is a recycle from Process 6 and Process 7 to Process 4. Recycle usually occur in chemical complexes, which makes it a challenging problem to use a stochastic inventory approach to determine the optimal stock levels of this type of inventory systems.[46] With the proposed model that integrates process planning with inventory management, we can explicitly address this challenge and handle it with the direct optimization approach without the need of detailed flow analysis. We solve the problem with the nonconvex MINLP models (P1) and (P2) using GAMS/BARON with 0% optimality margin. In contrast to the previous examples, the optimal solutions of using the "ideal" case uncertainty propagation and the "worst" case uncertainty propagation are

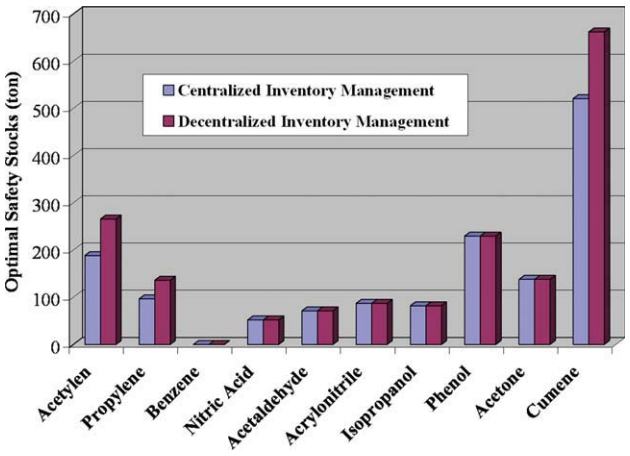

Figure 9. Optimal safety stocks for each chemical in Example 2 with centralized and decentralized inventory management.

[Color figure can be viewed in the online issue, which is available at wileyonlinelibrary.com.]

different for this example. Model (P1), which is for the "ideal" case uncertainty propagation, leads to a global minimum daily cost of $78,572.72/day, including $4652/day for safety stock cost, $7416.5/day for cycle stock cost, $34,717.5/day for production cost, and $31,786.7/day for purchase cost. Model (P2), which is for the "worst" case uncertainty propagation, leads to a global minimum daily cost of $78,581.70/day, including $4660.9/day for safety stock cost, $7416.5/day for cycle stock cost, $34,717.5/day for production cost, and $31,786.7/day for purchase cost. Note that in this case the difference between the "ideal" and "worst" case is very small.

The optimal production, purchase, sale, and inventory levels predicted by the two models are listed in Table 8 and Figures 11a, b. We can see that the optimal production, purchase and sale levels, and the cycle stock levels are the same for both solutions. In particular, Process 2 and Process 6 are operating with full capacity, whereas their parallel processes are not. The reason is that Process 2 has smaller unit production cost than Process 1, and Process 6 requires less feedstock than Process 7. In terms of inventory, it is interesting to note that the optimal solutions do not hold inventories for intermediates—Chemicals C, E, and F, to achieve the optimal inventory allocation. In addition, we can see from Figure 11b that the "worst" case approach leads to

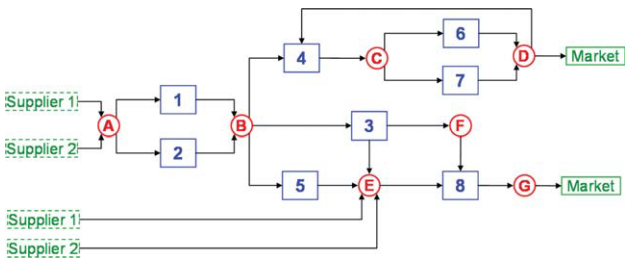

Figure 10. Example 3 with seven chemicals, eight processes, two suppliers, and one market.

[Color figure can be viewed in the online issue, which is available at wileyonlinelibrary.com.]

Table 7. Input Data of Example 3

	Production capacity Cap_i (ton/day)		
Process 1	60	Process 5	50
Process 2	50	Process 6	80
Process 3	90	Process 7	80
Process 4	90	Process 8	100
	Unit production cost δ_i ($/ton)		
Process 1	50	Process 5	50
Process 2	60	Process 6	90
Process 3	140	Process 7	75
Process 4	20	Process 8	100
	Production delay PD_i (day)		
Process 1	5	Process 5	5
Process 2	3	Process 6	4
Process 3	7	Process 7	2
Process 4	4	Process 8	4
	Unit inventory cost h_j ($/ton/day)		
A	1.5	E	6
B	5.5	F	8
C	7	G	5
D	5		
	Mass balance relationship		
Process 1	0.63 A → B		
Process 2	0.58 A → B		
Process 3	1.25 B → 4 C + E + 1.5 F		
Process 4	0.1 B + 0.05 D → C		
Process 5	0.8 B → E		
Process 6	2.04 C → D		
Process 7	2.3 C → D		
Process 8	0.93 E + 0.77 F → G		
	Γ_{jk}: unit purchase cost ($/ton)		
	A	E	
Supplier 1 (international)	550	567	
Supplier 2 (domestic)	820	840	
	SI_{jk}: guaranteed service time (day)		
	A	E	
Supplier 1 (international)	12	2	
Supplier 2 (domestic)	13	7	
	a_{jk}^{U}: upper bound of availability (ton/day)		
	A	E	
Supplier 1 (international)	60	50	
Supplier 2 (domestic)	100	100	

slightly higher safety stocks for Chemical A (272.87 tons vs. 266.91 tons), although the optimal cycle stocks are the same for both approaches. A comparison of the optimal VTM ratios with these two approaches is given in Figure 12. We can see that the ratios increase from downstream to upstream in both cases, and the ones for "ideal" case uncertainty propagation are always less than or equal to the ones for the "worst" case. Besides, the ratios are the same in both cases for the downstream chemicals and processes, but different for Chemicals A and B and Process 1 and Process 2. The reason is that the information flows of demand uncertainty from Chemical D and "cross" with the one from Chemical G at the chemical node B. Because of the two different ways of quantifying the upstream demand uncertainties, the optimal VTM ratios for Chemical B are different in the two cases, and the difference consequently affects the upstream chemical nodes and process nodes.

Table 8. Optimal Solution of the "Centralized" Inventory Management Instance in Example 2

	Production amount in terms of main product W_{ij_m} (ton/day)		
Process 1	45.71	Process 5	37.50
Process 2	50	Process 6	80
Process 3	46.20	Process 7	43.98
Process 4	79.55	Process 8	90
	Pu_{jk}: purchase amount (ton/day)		
	A	E	
Supplier 1 (international)	57.79	0	
Supplier 2 (domestic)	0	0	
	Sa_{jl}: sale amount to the market (ton/day)		
	D	G	
Market	120	90	
	Optimal cycle stock (ton)		
A	317.76	E	0
B	197.33	F	0
C	0	G	495
D	675.91		
	Optimal safety stock from Model (P1) (ton)		
A	266.91	E	0
B	212.76	F	0
C	0	G	340.57
D	275.72		
	Optimal safety stock from Model (P2) (ton)		
A	272.87	E	0
B	212.76	F	0
C	0	G	340.57
D	275.72		

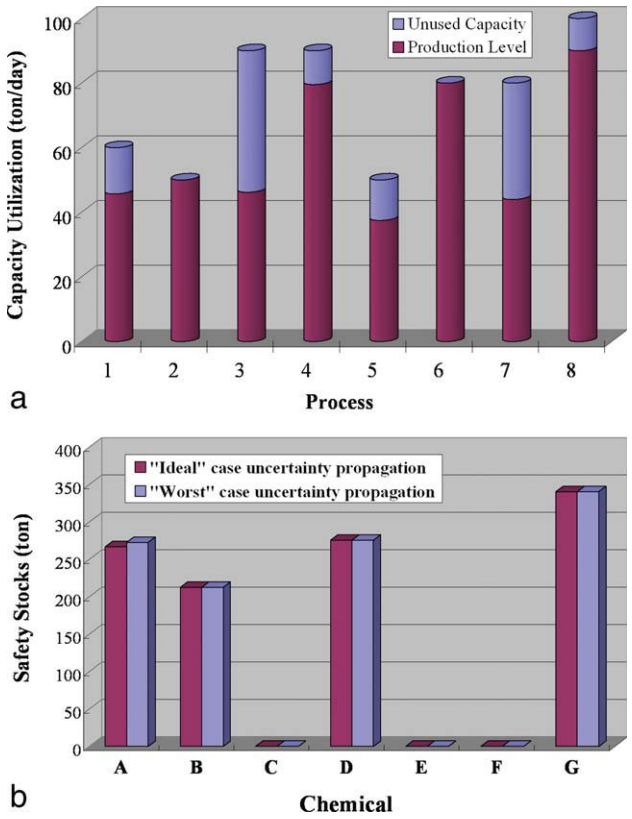

Figure 11. Optimal solution of Example 3 with seven chemicals, eight processes, two suppliers, and one market.

(a) Optimal production levels and unused capacities of each process for Example 3. (b) Optimal safety stock levels of Example 3 with two types of uncertainty propagation. [Color figure can be viewed in the online issue, which is available at wileyonlinelibrary.com.]

From this example, we can also see that there are not too many differences between the optimal solutions predicted by the "ideal" and "worst" case models. As model (P2) involves fewer nonconvex terms and represents the most conservative "worst" case, it can be used to deal with the large-scale problem for higher computational efficiency without sacrificing accuracy. In addition, the main purpose of holding inventory is to deal with the unexpected situation and account for the worst case. To this end, the "worst" case uncertainty propagation might be a more practical approach. In the next section, we first explore some properties of model (P2), and then present an efficient computational algorithm, followed by another two large-scale examples.

Solution Algorithm

Although small scale problems can be solved to global optimality effectively by using a global optimizer, medium and large-scale problems are often computationally intractable with a direct solution approach due to the combinatorial nature and nonlinear nonconvex terms. In this section, we present an effective solution algorithm based on the model properties and successive piecewise linear approximation to globally optimize (P2) with modest computational expense.

Reformulation

In model (P2) with the "worst" case uncertainty propagation, the only nonconvex constraint is (13), which involves the VTM ratio and the internal demand's variance. Although the linear constraints (15)–(17) can be used to define the VTM ratios under the worst case, we can get rid of these constraints and determine the ratios in a preoptimization step due to the following model property.

Property 1.

At the optimal solution of problem (P2), the optimal variance-to-mean ratios of internal demands, denoted as (RC_j^*, RP_i^*) *must be equal to one of the variance-to-mean ratios of the final demands* $\overline{R}_{jl}$. *In other words, at the optimum* $\exists\ j',l'$ *such that* $RC_j^* = \overline{R}_{j'l'}$, *and* $\exists\ j'',l''$ *such that* $RP_i^* = \overline{R}_{j''l''}$.

Proof. If there is a positive directed flow from the chemical node j to the chemical node j' which connects to market l', then due to the constraints (15)–(17), we can have $RC_j \geq \overline{R}_{j'l'}$. By figuring out all the possible flows that start from chemical node j and end at another chemical node j', which has positive uncertain demand in the external market l', we can have $RC_j \geq \overline{R}_{j'l'}$ for j and j' are on the same directed flow and $l' \in MKT(j')$. Thus, the lower bound of RC_j is given by $\max_{j',l' \in MKT(j')} \left\{\bar{R}_{j'l'}\right\}$. As the objective function is to

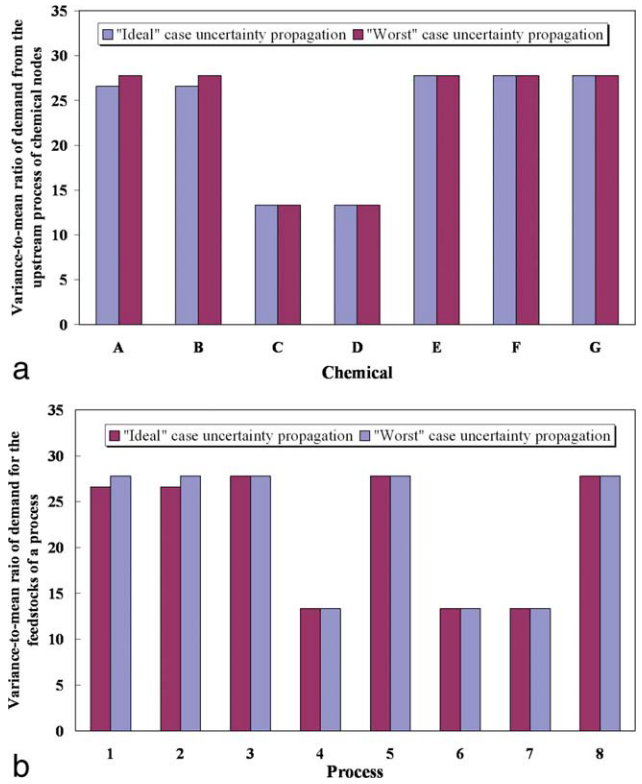

Figure 12. Variance-to-mean ratios propagate from downstream to upstream in Example 3.

(a) Variance-to-mean ratios of all the chemical nodes in Example 3. (b) Variance-to-mean ratios of all the process nodes in Example 3. [Color figure can be viewed in the online issue, which is available at wileyonlinelibrary.com.]

Table 9. Variance-to-Mean Ratios in Each Iteration

	Iter. 1	Iter. 2	Iter. 3	Iter. 4	Iter. 5	Iter. 6	Iter. 7	Iter. 8
RP_i								
Proc. 1	0	0	0	0	0	27.778	27.778	27.778
Proc. 2	0	0	0	0	0	27.778	27.778	27.778
Proc. 3	0	0	0	27.778	27.778	27.778	27.778	27.778
Proc. 4	0	0	0	13.333	13.333	13.333	13.333	13.333
Proc. 5	0	0	0	27.778	27.778	27.778	27.778	27.778
Proc. 6	0	13.333	13.333	13.333	13.333	13.333	13.333	13.333
Proc. 7	0	13.333	13.333	13.333	13.333	13.333	13.333	13.333
Proc. 8	0	27.778	27.778	27.778	27.778	27.778	27.778	27.778
RC_j								
A	0	0	0	0	0	0	27.778	27.778
B	0	0	0	0	27.778	27.778	27.778	27.778
C	0	0	13.333	13.333	13.333	13.333	13.333	13.333
D	13.333	13.333	13.333	13.333	13.333	13.333	13.333	13.333
E	0	0	27.778	27.778	27.778	27.778	27.778	27.778
F	0	0	27.778	27.778	27.778	27.778	27.778	27.778
G	27.778	27.778	27.778	27.778	27.778	27.778	27.778	27.778

minimize the total cost, including the safety stock cost, whereas a larger VTM ratio implies a higher variance of an internal demand, and consequently higher safety stock cost. Therefore, we can conclude that the optimal VTM ratio should lie at on its lower bound defined by the uncertainty propagation, i.e., $RC_j^* = \max_{j',l' \in MKT(j')}\{\bar{R}_{j'l'}\}$. Using a similar approach, one can show that $RP_i^* = \max_{j'',l'' \in MKT(j'')}\{\bar{R}_{j''l''}\}$ for i and j'' are on the same directed flow and $l'' \in MKT(j'')$. ■

Based on Property 1, we can determine the optimal VTM ratios in a preoptimization step. Various path-search algorithms can be implemented to handle this issue. Alternatively, one can use the following algorithm that requires at most $\max\{|i|, |j|\}$ iterations.

Step 1. Initialize iter = 1, $RP_i^{iter} = 0$, $RC_j^{iter} = 0$.
If $MKT(j) \neq \varnothing$, set $RC_j^{iter} = \max_{l \in MKT(j)}\{\bar{R}_{jl}\}$.

Step 2. For all i, j such that $i \in O(j)$,
$RP_i^{iter+1} = \max\{RP_i^{iter}, RC_j^{iter}\}$

Step 3. For all i, j such that $i \in I(j)$,
$RC_j^{iter+1} = \max\{RP_i^{iter}, RC_j^{iter}\}$

Step 4. For all j such that $MKT(j) \neq \varnothing$,
$RC_j^{iter+1} = \max\{RC_j^{iter+1}, \max_{l \in MKT(j)}\{\bar{R}_{jl}\}\}$

Step 5. Evaluate $diff = \sum_j (RC_j^{iter+1} - RC_j^{iter})^2 + \sum_i (RP_i^{iter+1} - RP_i^{iter})^2$.

Step 6. If $diff \leq 10^{-6}$, then set $RC_j^* = RC_j^{iter+1}$ and $RP_i^* = RP_i^{iter+1}$, and stop. Else, set iter = iter + 1 and go to Step 2.

For instance, applying this algorithm to Example 3, of which the chemical process network is given in Figure 10, requires eight iterations. The values of RC_j and RP_i at each iteration are given in Table 9.

With Property 1, we can determine the VTM ratios before solving the MINLP model (P2) and avoid the bilinear constraint (13). The second property of this model is about the timing relationship and is as follows.

Property 2.

Denote M as the maximum positive value such that for all the "timing" parameters PD_i, SI_{jk}, SO_{jl}^U, γ_{ij}, θ_{ij}, *have integer values for* PD_i/M, SI_{jk}/M, SO_{jl}^U/M, γ_{ij}/M, θ_{ij}/M, *then at the optimal solution of (P2), all the optimal net lead times, denoted as* $(N_{ij}^*, \overline{N}_{jl}^*)$ *also have integer values for* N_{ij}^*/M *and* $\overline{N}_{jl}^*/M$.

Proof. Since PD_i/M, SI_{jk}/M, SO_{jl}^U/M, γ_{ij}/M, θ_{ij}/M are all integers, the stochastic lead time constraints (1)–(7) can be reformulated as follows:

$$\frac{TP_i}{M} - \frac{SC_{ij}}{M} \geq \frac{\theta_{ij}}{M} + \frac{PD_i}{M}, \quad \forall j, \quad i \in I(j) \tag{A1}$$

$$\frac{SP_{ij}}{M} = \frac{TP_i}{M}, \quad \forall j, \quad i \in O(j) \tag{A2}$$

$$\frac{TC_j}{M} - \frac{SP_{ij}}{M} \geq \frac{\gamma_{ij}}{M}, \quad \forall j, \quad i \in O(j) \tag{A3}$$

$$\frac{TC_j}{M} \geq X_{jk} \cdot \frac{SI_{jk}}{M}, \quad \forall j, \quad k \in SUP(j) \tag{A4}$$

$$\frac{SC_{ij}}{M} \geq \frac{TC_j}{M} - \frac{N_{ij}}{M}, \quad \forall j, \quad i \in I(j) \tag{A5}$$

$$\frac{SO_{jl}}{M} \geq \frac{TC_j}{M} - \frac{\bar{N}_{jl}}{M}, \quad \forall j, \quad l \in MKT(j) \tag{A6}$$

$$\frac{SO_{jl}}{M} \leq \frac{SO_{jl}^U}{M}, \quad \forall j, \quad l \in MKT(j) \tag{A7}$$

As the right hand side of constraints (1), (3), (4), and (7) are all integers, these stochastic lead time constraints define an integral polyhedron with all the extreme points (N_{ij}^*/M, $\overline{N}_{jl}^*/M$, SO_{jl}^*/M, SC_{ij}^*/M, SP_{ij}^*/M, TC_j^*/M, TP_i^*/M) on the integer values. Note that these are the only constraints in model (P2) that relate to net lead time variables N_{ij} and $\overline{N}_{jl}$. Besides, if we fix all the production, purchase, and sale variables, the objective function is concave for variables (N_{ij}/M) and ($\overline{N}_{jl}/M$).[35] Similarly to the problem addressed by You and Grossmann,[35] this is a concave minimization problem over an integer polyhedron. Thus, the optimal solution always lies on the integer extreme points,[47,48] i.e., N_{ij}^*/M and $\overline{N}_{jl}^*/M$ must be integers. ■

Property 2 allows us to restrict N_{ij}/M to be on integer values. Each integer variable N_{ij}/M can be represented by a set of binary variables as follows[49]:

$$N_{ij} = M \cdot \sum_m 2^{|m|-1} \cdot Z_{ijm}, \quad \forall j, \quad i \in I(j) \tag{21.1}$$

$$Z_{ijm} \in \{0,1\}, \quad \forall j, m, \quad i \in I(j) \tag{21.2}$$

where Z_{ijm} determines the value of the mth digit of the binary representation of N_{ij}/M. Note that the upper bound of m depends on the upper bound of N_{ij} and the value of M, which also depends on the timing parameters. For example, if $N_{ij}^{\mathrm{U}} = 50$ and $M = 1$, we can set $m = 1, 2, 3, 4, 5$, and 6.

With this transformation, we can reformulate model (P2) to reduce the nonlinearities. Substituting (21) into the objective function (19), it can then be reformulated as follows.

$$\begin{aligned}\min \quad & \sum_i \sum_{j \in M_i} \delta_i \cdot W_{ij} + \sum_k \sum_{j \in \mathrm{SUP}(k)} \Gamma_{jk} \cdot \mathrm{Pu}_{jk} \\ & + \sum_j \frac{h_j}{2} \cdot \left(\sum_{l \in \mathrm{MKT}(j)} \bar{N}_{jl} \cdot \bar{\mu}_{jl} + M \cdot \sum_{i \in I(j)} \sum_m 2^{|m|-1} \cdot W_{ij} \cdot Z_{ijm} \right) \\ & + \sum_j \left(h_j \cdot \lambda_j \sqrt{\sum_{l \in \mathrm{MKT}(j)} \bar{N}_{jl} \cdot \bar{V}_{jl} + M \cdot \sum_{i \in I(j)} \sum_m 2^{|m|-1} \cdot Z_{ijm} \cdot V_{ij}} \right)\end{aligned} \tag{22}$$

Two non-negative variables G_j and Q_j are introduced as follows.

$$G_j = \sum_{l \in \mathrm{MKT}(j)} \bar{N}_{jl} \cdot \bar{V}_{jl} + M \cdot \sum_{i \in I(j)} \sum_m 2^{|m|-1} \cdot Z_{ijm} \cdot V_{ij}, \quad \forall j \tag{23}$$

$$Q_j = \sum_{l \in \mathrm{MKT}(j)} \bar{N}_{jl} \cdot \bar{\mu}_{jl} + M \cdot \sum_{i \in I(j)} \sum_m 2^{|m|-1} \cdot W_{ij} \cdot Z_{ijm}, \quad \forall j \tag{24}$$

Then the objective function can be further reformulated to (25) as follows.

$$\begin{aligned}\min \quad & \sum_i \sum_{j \in M_i} \delta_i \cdot W_{ij} + \sum_k \sum_{j \in \mathrm{SUP}(k)} \Gamma_{jk} \cdot \mathrm{Pu}_{jk} \\ & + \sum_j \frac{h_j}{2} \cdot Q_j + \sum_j \left(h_j \cdot \lambda_j \cdot \sqrt{G_j} \right)\end{aligned} \tag{25}$$

The linearization[50] of $(Z_{ijm} \cdot V_{ij})$ in constraint (23) requires two new continuous non-negative variable ZV_{ijm} and $\mathrm{ZV1}_{ijm}$, and the following constraints,

$$\mathrm{ZV}_{ijm} + \mathrm{ZV1}_{ijm} = V_{ij}, \quad \forall j, m, \quad i \in I(j) \tag{26.1}$$

$$\mathrm{ZV}_{ijm} \le V_{ij}^{\mathrm{U}} \cdot Z_{ijm}, \quad \forall j, m, \quad i \in I(j) \tag{26.2}$$

$$\mathrm{ZV1}_{ijm} \le V_{ij}^{\mathrm{U}} \cdot \left(1 - Z_{ijm}\right), \quad \forall j, m, \quad i \in I(j) \tag{26.3}$$

$$\mathrm{ZV}_{ijm} \ge 0, \quad \mathrm{ZV1}_{ijm} \ge 0, \quad \forall j, m, \quad i \in I(j) \tag{26.4}$$

where constraints (26.2), (26.3), and (26.4) ensure that if Z_{ijm} is zero, ZV_{ijm} should be zero; if Z_{ijm} is one, $\mathrm{ZV1}_{ijm}$ should be zero. Combining with constraint (26.1), we can have SZ_{jk} equivalent to the product of S_j and Z_{jk}.

Similarly, the nonlinear terms $(W_{ij} \cdot Z_{ijm})$ in (24) can be linearized as follows,

$$\mathrm{ZW}_{ijm} + \mathrm{ZW1}_{ijm} = W_{ij}, \quad \forall j, m, \quad i \in I(j) \tag{27.1}$$

$$\mathrm{ZW}_{ijm} \le W_{ij}^{\mathrm{U}} \cdot Z_{ijm}, \quad \forall j, m, \quad i \in I(j) \tag{27.2}$$

$$\mathrm{ZW1}_{ijm} \le W_{ij}^{\mathrm{U}} \cdot \left(1 - Z_{ijm}\right), \quad \forall j, m, \quad i \in I(j) \tag{27.3}$$

$$\mathrm{ZW}_{ijm} \ge 0, \ \mathrm{ZW1}_{ijm} \ge 0, \quad \forall j, m, \quad i \in I(j) \tag{27.4}$$

where ZW_{ijm} and $\mathrm{ZW1}_{ijm}$ are two new continuous variables.

Thus, constraints (23) and (24) can be replaced with the following equations.

$$G_j = \sum_{l \in \mathrm{MKT}(j)} \bar{N}_{jl} \cdot \bar{V}_{jl} + M \cdot \sum_{i \in I(j)} \sum_m 2^{|m|-1} \cdot \mathrm{ZV}_{ijm}, \quad \forall j \tag{28}$$

$$Q_j = \sum_{l \in \mathrm{MKT}(j)} \bar{N}_{jl} \cdot \bar{\mu}_{jl} + M \cdot \sum_{i \in I(j)} \sum_m 2^{|m|-1} \cdot \mathrm{ZW}_{ijm}, \quad \forall j \tag{29}$$

With the above equations, we can reformulate model (P2) with a new model, denoted as (P3), which includes the objective function (25) and constraints (1)–(13), (18), (21), and (26)–(29). Note that the value of RP_i in constraint (13) is predetermined, and thus, all the constraints are linear in model (P3).

Piecewise linear approximation

After the reformulation and linearization, we have the new model (P3) with all the constraints linear. The only nonlinear terms are in the objective function as univariate square root terms, $\sqrt{G_j}$. To improve the computational efficiency, we consider a piecewise linear approximation for the concave square root terms. There are several different approaches to model piecewise linear functions for a concave term. In this work, we use the "multiple-choice" formulation[51–54] to approximate the square root term $\sqrt{G_j}$. Let $P_j = \{1,2,3,\ldots, p\}$ denote the set of intervals in the piecewise linear function $\varphi(G_j)$, and $u_{j,0}$, $u_{j,1}$, $u_{j,2}$,… $u_{j,p}$, be the lower and upper bounds of G_j for each interval. The "multiple choice" formulation of $\varphi(G_j) = \sqrt{G_j}$ is given by,

$$\varphi(G_j) = \min \sum_p \left(\beta_{jp} E_{jp} + \alpha_{jp} F_{jp} \right) \tag{30}$$

s.t.

$$\sum_p E_{jp} = 1 \tag{31}$$

$$\sum_p F_{jp} = G_j \tag{32}$$

$$u_{j,p-1} E_{j,p} \le F_{j,p} \le u_{j,p} E_{j,p}, \quad \forall p \tag{33}$$

$$E_{j,p} \in \{0,1\}, \quad F_{jp} \ge 0, \quad \forall p \tag{34}$$

where $\alpha_{j,p} = \frac{\sqrt{u_{j,p}} - \sqrt{u_{j,p-1}}}{u_{j,p} - u_{j,p-1}}$ and $\beta_{j,p} = \sqrt{u_{j,p}} - \alpha_{j,p} u_{j,p}$, $p \in P$.

Substituting (30) into the objective function (25) yields a mixed-integer linear programming (MILP) model (P4), which

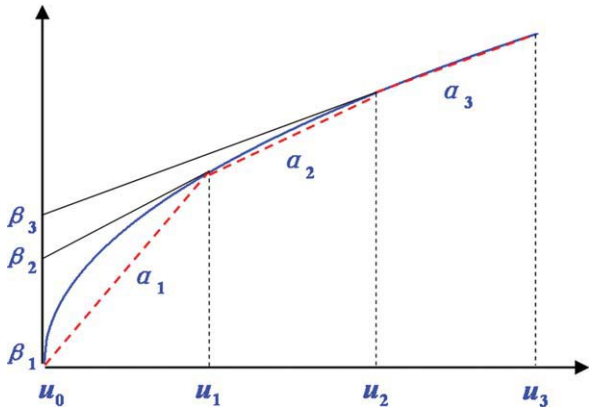

Figure 13. Piecewise linear under-estimator of a concave term.

[Color figure can be viewed in the online issue, which is available at wileyonlinelibrary.com.]

is piecewise linear under-estimator of the MINLP model (P3). The model formulation of (P4) is given as follows.

$$\min \quad \sum_i \sum_{j \in M_i} \delta_i W_{ij} + \sum_k \sum_{j \in \mathrm{SUP}(k)} \Gamma_{jk} \mathrm{Pu}_{jk} + \sum_j \frac{h_j Q_j}{2} + \sum_j \left(h_j \lambda_j \sum_p (\beta_{jp} E_{jp} + \alpha_{jp} F_{jp}) \right) \quad (35)$$

s.t. Constraints (1)–(13), (18), (21), (26)–(29), and (31)–(34).

Branch-and-refine algorithm

To globally optimize the nonconvex MINLP problem (P3), we can first solve the MILP problem (P4), whose solution provides a valid lower bound of the global optimal solution, and then solve a reduced nonlinear programming (NLP) problem by fixing the binary variables X_{jk} and Z_{ijm}. As the optimal solution of the reduced NLP is also a feasible solution of (P3), its objective value provides a valid global upper bound of the MINLP problem (P3). The remaining challenge is how to iteratively refine and improve the solution so that the global optimal solution can be obtained after a finite number of iterations. As can be seen in Figure 13, the more intervals that are used in (P4), the better is the approximation of the nonlinear concave function $\sqrt{G_j}$, but more additional variables and constraints are required. To control the size of problem (P3), we use an iterative branch-and-refine strategy based on successive piecewise linear approximation.

In the first step of this algorithm, we consider a one-piece linear approximation in (P4), i.e., replacing all the square root terms in (P3) with their secants as shown in Figure 14a. Thus, the optimal solution of the MILP problem (P4) provides the first lower bound LB1. Note that the optimal solution of (P4) is also a feasible solution of the MINLP problem (P3). Thus, an upper bound can be obtained by, (a) substituting the optimal solution of (P3) into (P4) and directly evaluate the objective function or (b) fixing the values of the binary variables X_{jk} and Z_{ijm} and then solve the reduced NLP problem of (P4). Solving the reduced NLP may provide a better solution, but sometimes the NLP subproblems might become infeasible due to numerical difficulties. Thus, we use a combined approach: First, solve the reduced NLP; if it is feasible and return optimal solution, we move on to the next's step; if not, we use function evaluation with the optimal solution from (P4). The combined approach allows us to obtain an upper bound in each iteration, regardless if the reduced NLP is feasible or not.

In the next step, we use the optimal solution of variable G_j in the upper bounding problem as the lower bound of a new interval, and consider a two-interval linear approximation of the square root terms as shown in Figure 14b. Note that for those $\sqrt{G_j}$, the optimal solution of the upper

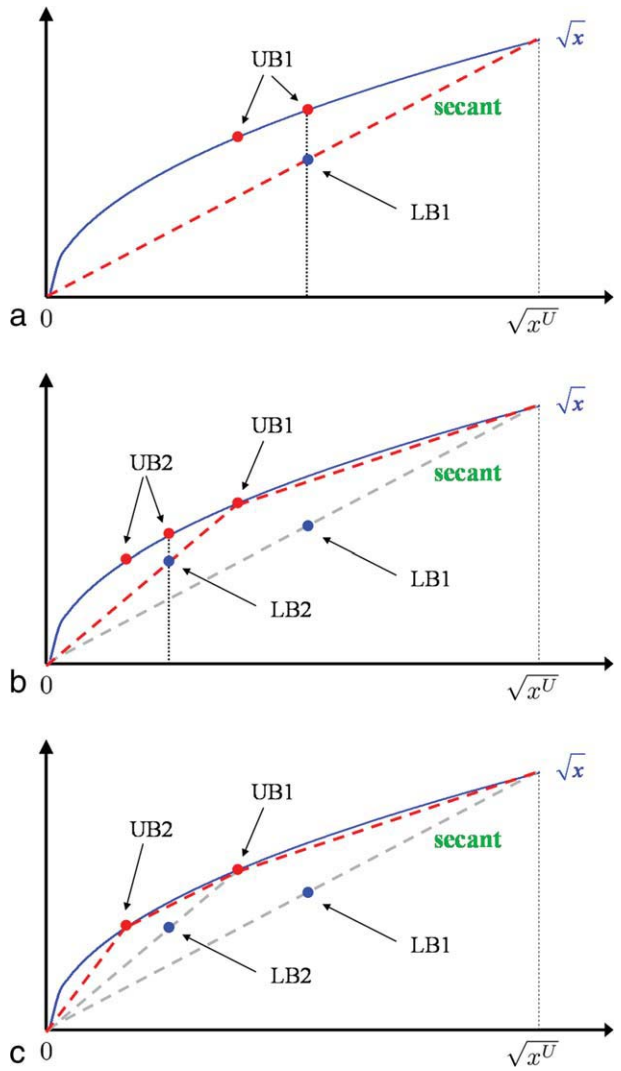

Figure 14. Branch-and-refine algorithm based on successive piecewise linear approximation.

(a) Iteration 1—replace the square root terms with their secant, the optimal solution of the MILP provides a lower bound LB1, and the upper bound can be obtained from function evaluation or from solving the reduced NLP. (b) Iteration 2—add a new interval based on the optimal solution of the upper bounding problem in Iteration 1, and consider a two-piece linear approximation of the square root terms. (c) Iteration 3—add another new interval based on the optimal solution of the upper bounding problem in the previous iteration. [Color figure can be viewed in the online issue, which is available at wileyonlinelibrary.com.]

bounding problem in the previous iteration lies at the bounds of some intervals, then we do not add a new interval for these square root terms. After we construct the two-interval linear approximation MILP model (P4), we can similarly obtain a lower bound, and then an upper bound by function evaluation or solving the reduced NLP.

As shown in Figure 14c, as the iteration number increases, the number of intervals increases in (P4), and the best lower bound increases, whereas the best upper bond decreases. The algorithm keeps iterating until the lower bound and upper bound are close enough to reach an optimality tolerance, e.g., 10^{-6}. Note that the number of intervals does not always equal to the number of iterations, because the optimal solutions in some iterations may lie at the bounds of the intervals and in that case we do not add a new interval to the MILP relaxation of the corresponding square root terms.

To summarize, the proposed branch-and-refine algorithm based on successive piecewise linear approximation is as follows:

Step 1 (Initialization). Set iter = 1, LB = 0, UB = $+\infty$. Set $NP_j^{iter} = 1$ and $p \in P_j = \{0,1,\ldots,NP_j^{iter}\}$. Construct one-interval linear approximation, i.e., the secant, of the square root terms. To achieve this, we set $u_{j,0} = 0$ and $u_{j,1} = G_j^U$, as well as $\alpha_{j,1} = \frac{\sqrt{u_{j,1}} - \sqrt{u_{j,0}}}{u_{j,1} - u_{j,0}} = \frac{1}{\sqrt{G_j^U}}$ and $\beta_{j,1} = \sqrt{u_{j,1}} - \alpha_{j,1} u_{j,1} = 0$.

Step 2. At iteration *iter*, solve the piecewise linear approximation MILP model (P4). Denote the optimal objective function value as φ^{iter} and the optimal solution of variables X_{jk} and Z_{ijm} as (X_{jk}^{*iter}, Z_{ijm}^{*iter}). Fix the values of binary variables $X_{jk} = X_{jk}^{*iter}$ and $Z_{ijm} = Z_{ijm}^{*iter}$, and solve the original model (P3) in the reduced space as an NLP to obtain the local optimal objective function Φ^{iter} and optimal solution G_j^{iter}. If the reduced NLP problem (P3) is infeasible, then substitute the optimal solution of the MILP problem into the original model (which is always feasible) and evaluate the objective function value as Φ^{iter} and optimal solution G_j^{iter}.

Step 3. If $\Phi^{iter} <$ UB, then set UB = Φ^{iter}, store the current optimal solution of the (P3). If the NLP is infeasible, store the optimal solution of the MILP model (P4).

If $\varphi^{iter} >$ LB, then set LB = φ^{iter}.

Find n_j^{iter} such that the optimal solution G_j^{iter} lies in the n_j^{iter}th interval, i.e., $u_{j,n_j^{iter}-1} \le G_j \le u_{j,n_j^{iter}}$. One approach to find the proper n_j^{iter} is to compute the product $(G_j^{iter} - u_{j,p-1}) \cdot (G_j^{iter} - u_{j,p})$ for all the $p = 2, 3, \ldots, NP_j^{iter}$, and then denote the first p that leads to a nonpositive value (zero or negative value) of the product as n_j^{iter}, i.e., if $(G_j^{iter} - u_{j,p-1}) \cdot (G_j^{iter} - u_{j,p}) \le 0$, set $n_j^{iter} = p$.

If UB − LB $\le \varepsilon$ (e.g., 10^{-9}), stop and output the optimal solution; otherwise, go to the next step.

Step 4. For those $j \in J$ such that $G_j^{iter} = u_{j,n_j^{iter}}$, set $NP_j^{iter+1} = NP_j^{iter}$, $u_{j,p}^{iter+1} = u_{j,p}^{iter}$, $\alpha_{j,p}^{iter+1} = \alpha_{j,p}^{iter}$, and $\beta_{j,p}^{iter+1} = \beta_{j,p}^{iter}$.

For other $j \in J$, set $NP_j^{iter+1} = NP_j^{iter} + 1$ and update set P_j, i.e., $p \in P_j = \{0,1,\ldots,NP_j^{iter}, NP_j^{iter+1}\}$. Then update $u_{j,p}$, $\alpha_{j,p}$, and $\beta_{j,p}$ as follows:

(a) For $p < n_j^{iter}$ (i.e., $p = 0, 1, 2 \ldots, n_j^{iter} - 1$), set $u_{j,p}^{iter+1} = u_{j,p}^{iter}$, $\alpha_{j,p}^{iter+1} = \alpha_{j,p}^{iter}$, and $\beta_{j,p}^{iter+1} = \beta_{j,p}^{iter}$.

(b) For $p = n_j^{iter}$, set $u_{j,n_j^{iter}}^{iter+1} = G_j^{iter}$, $\alpha_{j,n_j^{iter}}^{iter+1} = \frac{\sqrt{G_j^{iter}} - \sqrt{u_{j,n_j^{iter}-1}}}{G_j^{iter} - u_{j,n_j^{iter}-1}}$, and $\beta_{j,n_j^{iter}}^{iter+1} = \sqrt{G_j^{iter}} - \alpha_{j,n_j^{iter}}^{iter+1} \cdot G_j^{iter}$

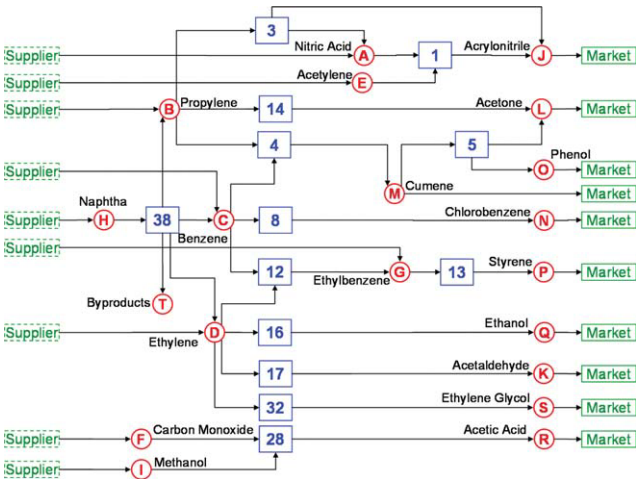

Figure 15. Example 4 with 20 chemicals, 13 processes, two suppliers, and one market.

[Color figure can be viewed in the online issue, which is available at wileyonlinelibrary.com.]

(c) For $p = n_j^{iter} + 1$, set $u_{j,n_j^{iter}+1}^{iter+1} = u_{j,n_j^{iter}}^{iter}$, $\alpha_{j,n_j^{iter}+1}^{iter+1} = \frac{\sqrt{u_{j,n_j^{iter}}} - \sqrt{G_j^{iter}}}{u_{j,n_j^{iter}} - G_j^{iter}}$, and $\beta_{j,n_j^{iter}+1}^{iter+1} = \sqrt{u_{j,n_j^{iter}}} - \alpha_{j,n_j^{iter}+1}^{iter+1} \cdot u_{j,n_j^{iter}}$

(d) For $p > n_j^{iter} + 1$ (i.e., $p = n_j^{iter} + 2$, $n_j^{iter} + 3$, …, NP_j^{iter}), set $u_{j,p}^{iter+1} = u_{j,p-1}^{iter}$, $\alpha_{j,p}^{iter+1} = \alpha_{j,p-1}^{iter}$, and $\beta_{j,p}^{iter+1} = \beta_{j,p-1}^{iter}$.

Then, set iter = iter + 1 and go to Step 2.

We should note that the entire procedure requires only an MILP solver. An NLP solver can be used to solve the upper bounding problem in the reduced variable space in Step 2, but it is not necessary. The reason is that the solution of the nonlinear optimization problem (P3), which reduces to an NLP from MINLP after X_{jk} and Z_{ijm} are fixed, can be substituted by simple function evaluation as stated in Step 2, although the solution quality may be sacrificed.

Computational Results

To illustrate the performance of the proposed solution strategies, we consider two large-scale problems, Examples 4 and 5. All the computational experiments are performed on an IBM T400 laptop with Intel 2.53 GHz CPU and 2 GB RAM. The proposed solution procedure is coded in GAMS 23.2.1.[44] The MILP problems are solved using CPLEX 12, the NLP problems in Step 2 of the branch-and-refine algorithm are solved with solver KNITRO 6.0.0. We use DICOPT as the convex MINLP solver and the global optimizer used in the computational experiments is BARON 8.1.5. The optimality tolerances of DICOPT, BARON, and the proposed algorithm are all set to 10^{-6} and optimality margins of solving the piecewise linear approximation MILP model (P4) and the reduced NLP model (P3) are both 10^{-9}.

Example 4: Computational performance, inventory allocation

To test the performance of the proposed algorithm, we consider Example 4, which has 20 chemicals, 13 processes.

Table 10. Input Data of the First Instance of Example 4 (1 Supplier and 1 Market)

	Production capacity Cap_i (ton/day)		
Process 1	15	Process 14	100
Process 3	150	Process 16	150
Process 4	180	Process 17	50
Process 5	90	Process 28	50
Process 8	50	Process 32	250
Process 12	50	Process 38	120
Process 13	40		
	Unit production cost δ_i ($/ton)		
Process 1	80	Process 14	200
Process 3	120	Process 16	100
Process 4	150	Process 17	130
Process 5	110	Process 28	100
Process 8	250	Process 32	200
Process 12	70	Process 38	100
Process 13	70		
	Production delay PD_i (day)		
Process 1	2	Process 14	3
Process 3	3	Process 16	2
Process 4	2	Process 17	4
Process 5	4	Process 28	5
Process 8	5	Process 32	4
Process 12	4	Process 38	3
Process 13	2		
	List of chemicals		
A	Nitric acid	K	Acetaldehyde
B	Propylene	L	Acetone
C	Benzene	M	Cumene
D	Ethylene	N	Chlorobenzene
E	Acetylene	O	Phenol
F	Carbon monoxide	P	Styrene
G	Ethylbenzene	Q	Ethanol
H	Naphtha	R	Acetic acid
I	Methanol	S	Ethylene glycol
J	Acrylonitrile	T	Byproducts

		Unit inventory cost h_j ($/ton/day)					
A	1.5	F	8.0	K	1.5	P	8.0
B	2.5	G	5.0	L	2.5	Q	5.0
C	3.0	H	5.0	M	3.0	R	3.0
D	5.0	I	7.0	N	5.0	S	7.0
E	6.0	J	2.0	O	10	T	2.0

	Mass balance relationship
Process 1	0.58 Nitric acid → 0.63 acetylene + acrylonitrile
Process 3	1.25 Propylene → 0.055 nitric acid + acrylonitrile
Process 4	0.40 Propylene + 0.69 benzene → cumene
Process 5	2.3 Cumene → acetone + 1.7 phenol
Process 8	Benzene → chlorobenzene
Process 12	0.76 Benzene + 0.28 ethylene → ethylbenzene
Process 13	1.14 Ethylbenzene → styrene
Process 14	0.78 Propylene → acetone
Process 16	0.60 Ethylene → ethanol
Process 17	0.67 Ethylene → acetaldehyde
Process 28	0.56 Carbon monoxide + 0.56 methanol → acetic acid
Process 32	0.53 Ethylene → ethylene glycol
Process 38	3.08 Naphtha → 0.38 propylene + 0.22 benzene + ethylene + 1.81 byproducts

(*Continued*)

Table 10. (Continued)

	$\overline{\mu}_{jl}$: mean value of demands of Market 1 (ton/day)		
Acrylonitrile	150	Styrene	25
Acetaldehyde	30	Ethanol	70
Acetone	30	Acetic acid	30
Cumene	80	Ethylene glycol	250
Chlorobenzene	30	Byproducts	250
Phenol	70		
	$\overline{\sigma}_{jl}$: standard deviation of demands of Market 1 (ton/$\sqrt{}$day)		
Acrylonitrile	50	Styrene	5
Acetaldehyde	10	Ethanol	20
Acetone	10	Acetic acid	10
Cumene	20	Ethylene glycol	80
Chlorobenzene	10	Byproducts	70
	Γ_{jk}: unit purchase cost of Supplier 1($/ton)		
Nitric acid	820	Carbon monoxide	40
Propylene	400	Ethylbenzene	660
Benzene	440	Naphtha	410
Ethylene	350	Methanol	260
Acetylene	550		
	SI_{jk}: guaranteed service time of Supplier 1 (day)		
Nitric acid	8	Carbon monoxide	1
Propylene	4	Ethylbenzene	6
Benzene	4	Naphtha	4
Ethylene	5	Methanol	3
Acetylene	5		
	a_{jk}^{U}: upper bound of availability of Supplier 1 (ton/day)		
Nitric acid	200	Carbon monoxide	600
Propylene	225	Ethylbenzene	240
Benzene	300	Naphtha	990
Ethylene	200	Methanol	220
Acetylene	250		

The chemical process network of Example 4 is given in Figure 15. We consider 10 instances of this example, ranging from 1 supplier and 1 market instance to 10 supplier and 10 market instances.

The safety stock factors in all the instances are set to 2.0537, corresponding to 98% service level. All the external demands of chemicals in the market follow a normal distribution. The purchase lower bounds, the maximum GSTs of

Table 11. Problem Sizes for the 10 Instances of Example 4

Number of Suppliers	Number of Markets	MINLP Model (P2)			MILP Model (P4) for Piecewise linear Approximation (Largest Model Size)			Reduced (P3)—NLP (Largest Model Size)		Maximum Iterations
		Dis. Var.	Con. Var.	Const.	Dis. Var.	Con. Var.	Const.	Con. Var.	Const.	
1	1	9	212	238	179	746	1105	684	962	4
2	2	18	254	298	183	784	1144	716	1012	4
3	3	27	296	358	190	824	1188	746	1060	4
4	4	36	338	418	213	880	1266	778	1110	6
5	5	45	380	478	231	930	1332	808	1158	5
6	6	54	422	538	244	1220	1390	840	1208	5
7	7	63	464	598	246	1012	1424	870	1256	5
8	8	72	506	658	259	1058	1482	902	1306	5
9	9	81	548	718	262	1094	1518	932	1354	4
10	10	90	590	778	262	1126	1550	964	1404	6

Dis. Var., discrete variables; Con. Var., continues variable; Const., constraints.

Table 12. Comparison of the Performance of the Algorithms for the 10 Instances of Example 4

Number of Suppliers	Number of Markets	Solving MINLP Model (P2) with DICOPT Directly			Solving MINLP Model (P2) with BARON Directly				Proposed Algorithm		
		Solution	Time (s)	Gap	Solution	LB	Gap	Time (s)	Solution	Time (s)	Max. Iter.
1	1	537,891	0.8	0.92%	532,919	531,089	0.34 %	3,600	532,919	8.3	4
2	2	477,306*	3.5	0.05%	479,165	467,393	2.46%	3,600	477,051	3.5	4
3	3	485,200	4.5	0.06%	485,200	456,645	5.89%	3600	484,898	7.4	4
4	4	488,231	22.4	1.73%	482,855	459,065	4.93%	3600	479,770	52.4	6
5	5	496,636	14.8	2.11%	511,998	458,780	10.4%	3600	486,146	11.3	5
6	6	487,181	22.0	1.29%	508,040	455,821	10.3%	3600	480,918	18.3	5
7	7	496,736	20.1	6.19%	496,317	455,754	8.17%	3600	465,995	37.3	5
8	8	481,114*	42.9	0%	504,710	467,810	7.31%	3600	481,114	52.0	5
9	9	495,382	28.1	4.15%	497,375	457,441	8.03%	3600	474,814	38.4	4
10	10	524,721	67.4	10.7%	583,188	458,796	21.3%	3600	474,009	46.7	6

*Infeasible before adding a sufficient small number ε (e.g., 0.0001) under each square root terms in the objective function.

chemicals to the market, and the deterministic transfer times from process i to storage tank of chemical $j(\gamma_{ij})$ and from storage tank of chemical j to process $i(\theta_{ij})$ are all set to zero. The remaining input data for the first instance with one supplier and one market are given in Table 10. Input data for other instances are available upon request.

The problem sizes of all the 10 instances are listed in Table 11. For each instance, we first solve the original nonconvex MINLP model (P2) with MINLP solvers BARON and DICOPT directly, and then implement the proposed algorithm by iteratively solving the piecewise linear approximation MILP model (P4) with CPLEX and the reduced model (P3), which is an NLP after fixing the binary variables, with KNITRO. Note that for the MILP model (P4) and the reduced NLP model (P3) after fixing the binary variables, we only report the maximum problem sizes, i.e., the model sizes in the last iteration of the branch-and-refine algorithm. From Table 11, we can see that problem sizes of (P2) increases as the number of suppliers and markets increases. The maximum problems sizes of (P4) and (P3) also increase as the number of markets and suppliers increases, although the number of required iterations for the branch-and-refine algorithm does not strictly increases as the problems sizes increases.

The computational performance of DICOPT, BARON, and the proposed algorithm for these 10 instances are presented in Table 12. Note that there are two types of "Gap" in this table. The column "Gap" for solving (P2) with DICOPT is for the differences between the solutions obtained by using DICOPT and the global optimal solutions, which are obtained with the proposed algorithm. The "Gap" column for solving (P2) with BARON is for the differences between the lower and upper bounds returned by BARON. As we can see from Table 12, DICOPT can solve all the instances in less than 70 s, but usually leads to suboptimal solutions with relatively large global optimality margin (up to 10.7%) for large scale instances. For the second and the eighth instances, DICOPT was not able to return a feasible solution initially due to the numerical difficulty in its NLP subproblems. After adding a sufficiently small number ε (e.g., 0.0001) under all the square root terms in the objective function, we can avoid unbounded gradient in the NLP subproblems and obtain near-optimal solutions as shown in Table 12. When compared with DICOPT, the performance of

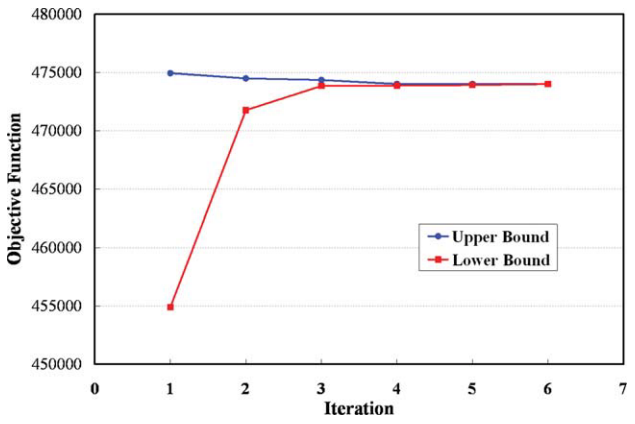

Figure 16. Bounds of each iteration of the proposed branch-and-refine algorithm Example 4 with 20 chemicals, 13 processes, 10 suppliers, and 10 markets.

[Color figure can be viewed in the online issue, which is available at wileyonlinelibrary.com.]

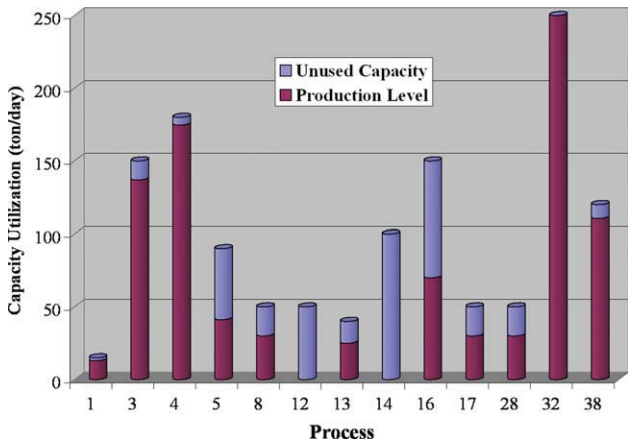

Figure 17. Optimal production levels and unused capacities of each process in the first instance of Example 4 with 20 chemicals, 13 processes, one supplier, and one market.

[Color figure can be viewed in the online issue, which is available at wileyonlinelibrary.com.]

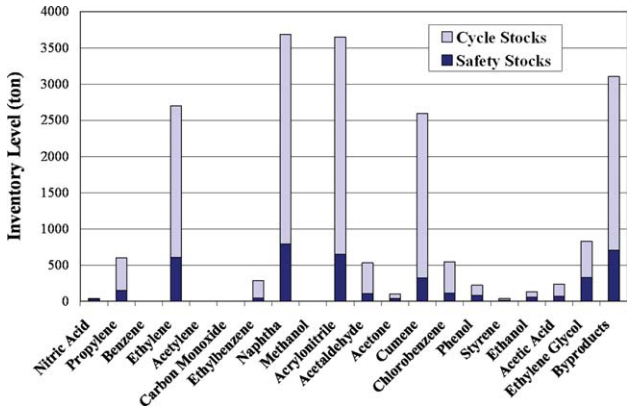

Figure 18. Optimal inventory levels of all the chemicals in the first instance of Example 4 with chemicals, 13 processes, one supplier, and one market.

[Color figure can be viewed in the online issue, which is available at wileyonlinelibrary.com.]

the global optimizer BARON is not very good—BARON could not globally optimize any of the 10 instances after running for 1 h, and most of the suboptimal solutions returned after 3600 CPUs have relatively large optimality gaps (in average around 10% and the maximum is 21.3%), although BARON does return feasible solutions for all the instances. When compared with solving (P2) with DICOPT and BARON directly, the proposed algorithm has a significantly better performance. Although the number of iterations may vary from instances to instances (usually 4–6 iterations), the total CPU times for iteratively solving the MILP problem (P4) and the reduced NLP problem (P3) with binary variables fixed are always less than 1 min for all the 10 instances. In addition, the proposed algorithm can guarantee global optimality with similar computational times required by DICOPT. The computational results suggest the significant advantage of using the proposed branch-and-refine algorithm for solving medium and large-scale instances. The change of bounds during the branch-and-refine algorithm for the largest instance with 10 suppliers and 10 markets are given in Figure 16. We can see that as iterations proceed, the lower bound keeps increasing, and the upper bound, which is the objective value of a feasible solution, keeps decreasing, until the termination criterion is satisfied. In particular, we can see that the upper bound obtained in the first iteration is rather close to the global optimal solution. Recall that we use the optimal solution of the MILP (P4) as the initial point for solving the NLP (P3) to obtain the upper bounds. The tight upper bound in the first iteration implies that replacing the square root terms in (P3) with the one-piece under-estimator, i.e., the secant, and then solving the resulting MILP problem can lead to very good initial point for solving the NLP, and potentially yield very tight upper bound of the original problem. Similar performance of this approach was also observed and discussed in You and Grossmann.[35]

The optimal solutions of the first instance of Example 4 with 20 chemicals, 13 processes, one supplier, and one market are given in Figures 17 and 18. Figure 17 shows the optimal production level in terms of the production amount of main product, and the unused production capacity of all the processes. We can see that Processes 1, 3, 4, 32, and 38 are operating with almost full capacity, Processes 5, 8, 13, 16, 17, and 28 are using around half of the capacity, whereas Processes 12 and 14 do not produce any product. The reason is that ethylbenzene is mainly purchased from the supplier instead of being produced from Process 12 due to the price advantage, and acetone is produced from Process 5 instead of Process 14 for lower production cost. Figure 18 shows the optimal inventory levels of all the 20 chemicals in the chemical process network. We can see that intermediates benzene and acetylene as well as feedstocks carbon monoxide and methanol have zero inventories, although their downstream chemicals hold sufficiently large safety stocks and cycle stocks. The results show that optimal inventory allocation is a highly nontrivial problem for large scale chemical complexes, and it is difficult to use a ''rule of thumb'' to make such decisions.

Table 13. List of Chemicals in Example 5

A	Nitric acid	O	Phenol
B	Propylene	P	Styrene
C	Benzene	Q	Ethanol
D	Ethylene	R	Acetic acid
E	Acetylene	S	Ethylene glycol
F	Carbon monoxide	T	Byproducts
G	Ethylbenzene	U	Vinyl acetate
H	Naphtha	V	Acetic anhydride
I	Methanol	W	Ethylene dichloride
J	Acrylonitrile	X	Ethylene glycol
K	Acetaldehyde	Y	Formaldehyde
L	Acetone	Z	Byproducts
M	Cumene	AA	Ketene
N	Chlorobenzene	AB	Ethylene chlorohydrin

Table 14. Problem Sizes for the 5 Instances of Example 5

Number of Suppliers	Number of Markets	MINLP Model (P2)			MILP Model (P4) for Piecewise Linear Approximation (Largest Model Size)			Reduced (P3)—NLP (Largest Model Size)		Maximum Iterations
		Dis. Var.	Con. Var.	Const.	Dis. Var.	Con. Var.	Const.	Con. Var.	Const.	
1	1	10	470	522	405	1864	2708	1788	2534	3
5	5	50	702	834	447	2098	2960	1956	2782	4
10	10	100	992	1224	494	2384	3264	2166	3092	3
15	15	150	1282	1614	538	2668	3562	2376	3402	2
20	20	200	1572	2004	588	2958	3872	2586	3712	2

Dis. Var., discrete variables; Con. Var., continues variable; Const., = constraints.

Table 15. Comparison of the Performance of the Algorithms for the 5 Instances of Example 5

Number of Suppliers	Number of Markets	Solving MINLP Model (P2) with DICOPT Directly			Solving MINLP Model (P2) with BARON Directly				Proposed Algorithm		
		Solution	Time (s)	Gap	Solution	LB	Gap	Time (s)	Solution	Time (s)	Max. Iter.
1	1	409,705*	42.8	2.96%	407,595	381,209	6.92%	3600	397,945	119.5	3
5	5	367,113*	88.9	5.80%	360,612	328,452	9.79%	3600	347,014	230.7	4
10	10	351,404*	81.2	1.79%	372,469	325,984	14.3%	3600	345,208	729.9	3
15	15	343,754*	105.4	1.93%	360,808	322,278	12.0%	3600	337,235	299.8	2
20	20	344,215*	247.5	2.27%	396,641	321,795	23.3%	3600	336,562	981.7	2

*Infeasible before adding a sufficient small number ε (e.g., 0.0001) under each square root terms in the objective function.

Example 5: Computational performance, responsiveness, and Pareto optimization

In the last example, let us consider the large-scale chemical process network discussed at the beginning of this article and shown in Figure 3. A list of all chemicals included in the chemical complex is given in Table 13. We still consider 98% service level for all the chemicals and the maximum GST to the external market are all set to zero. Because of the large size of the problem, the remaining input data are not listed here, but are all available upon request.

Similarly to the previous example, we consider 5 instances with different numbers of suppliers and markets. All the problem sizes are listed in Table 14 and the computational performance of the solvers and the proposed algorithm are shown in Table 15. Similar to what we observed in the previous example, the problem sizes increase as the number of suppliers and markets increases. For these large-scale instances, DICOPT failed to return any feasible solutions without adding a sufficient small number ε (e.g., 0.0001) in the square root terms of the objective function, due to numerical difficulty in the NLP subproblems. After the minor modification of the objective function, we can avoid unbounded gradients in the NLP subproblems and obtain near-optimal solutions (with optimality gap up to 5.8%) as shown in Table 15. The global optimizer BARON still yields relatively large gaps between the lower and upper bounds after running for 3600 s. However, the proposed algorithm is able to globally optimize all the instances with modest CPU times (less than 1000 s), and the number of iterations is still modest (2–4 iterations) so that the sizes of (P4) and reduced (P3) are not too large. All these five instances again show that the proposed algorithm is able to efficiently solve to global optimality the joint stochastic inventory management and tactical process planning problem, compared with the commercial MINLP solvers.

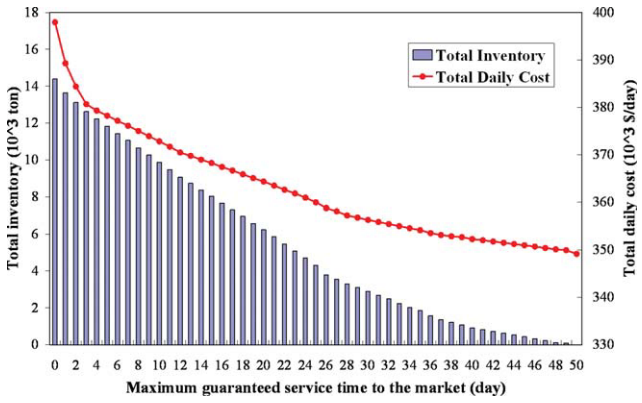

Figure 19. Pareto optimal curve and optimal inventory levels under different specifications of the maximum guaranteed service time to market for Example 5.

[Color figure can be viewed in the online issue, which is available at wileyonlinelibrary.com.]

In addition to illustrating the performance of the proposed algorithm, we address the "responsiveness" issue of this chemical complexes using an approach similar as the one discussed in You and Grossmann.[37] As the maximum GST of chemicals to external markets (SO^U_{jl}) is the measure of responsiveness, changing the values of this parameter will lead to changes of the optimal inventory levels and probably the optimal production, purchase, and sale levels as well. Thus, we generate 51 instances of this example (with the one supplier and one market instance) by fixing the parameter SO^U_{jl} to 51 values evenly distributed in [0, 50], i.e., 0, 1, 2, …, 49, 50. All the instances are then solved with the proposed algorithm. All the 51 instances require a total CPU time of 1716.5 s. The results produce a Pareto optimal curve shown in the line of Figure 19, which reveals the trade-off between the total daily cost and the measure of responsiveness, the maximum GST to the markets. We can see that as the maximum GST to the markets increases from 0 to 50 days, the optimal total daily cost decreases monotonically from $397,945/day to $349,145/day. In particular, there is a steep decrease of the optimal total daily cost from $397,945/day to $380,663/day when the maximum GST to the markets increases from 0 to 3 days. Thus, setting the maximum GST to the markets to 3 days might be a good choice in terms of balancing the economics and responsiveness. Similar to the total daily cost, the optimal total inventory also decreases monotonically from 14,391 tons to 0 ton, as the maximum GST to the markets increases from 0 to 50 days. However, the decreasing rate of the optimal inventory level does not strictly follow the one of the total daily cost. It implies that as maximum GST to the markets increases, not only the inventory levels but also the production, purchase, and sale activities change to reduce the total daily cost. Figures 20a–f show the optimal safety stocks and cycle stocks for all the chemicals under six different specifications of the maximum GST to the markets (0 day, 10 days, 20 days, 30 days, 40 days, and 50 days). There is a clear trend that as the maximum GST to the market increases, the inventories of all the chemicals decrease. In particular, we can see in Figure 20a that when the maximum GST to the markets is zero, it is optimal to hold sufficiently high inventories for the propylene, benzene, and ethylene, which are the major feedstocks

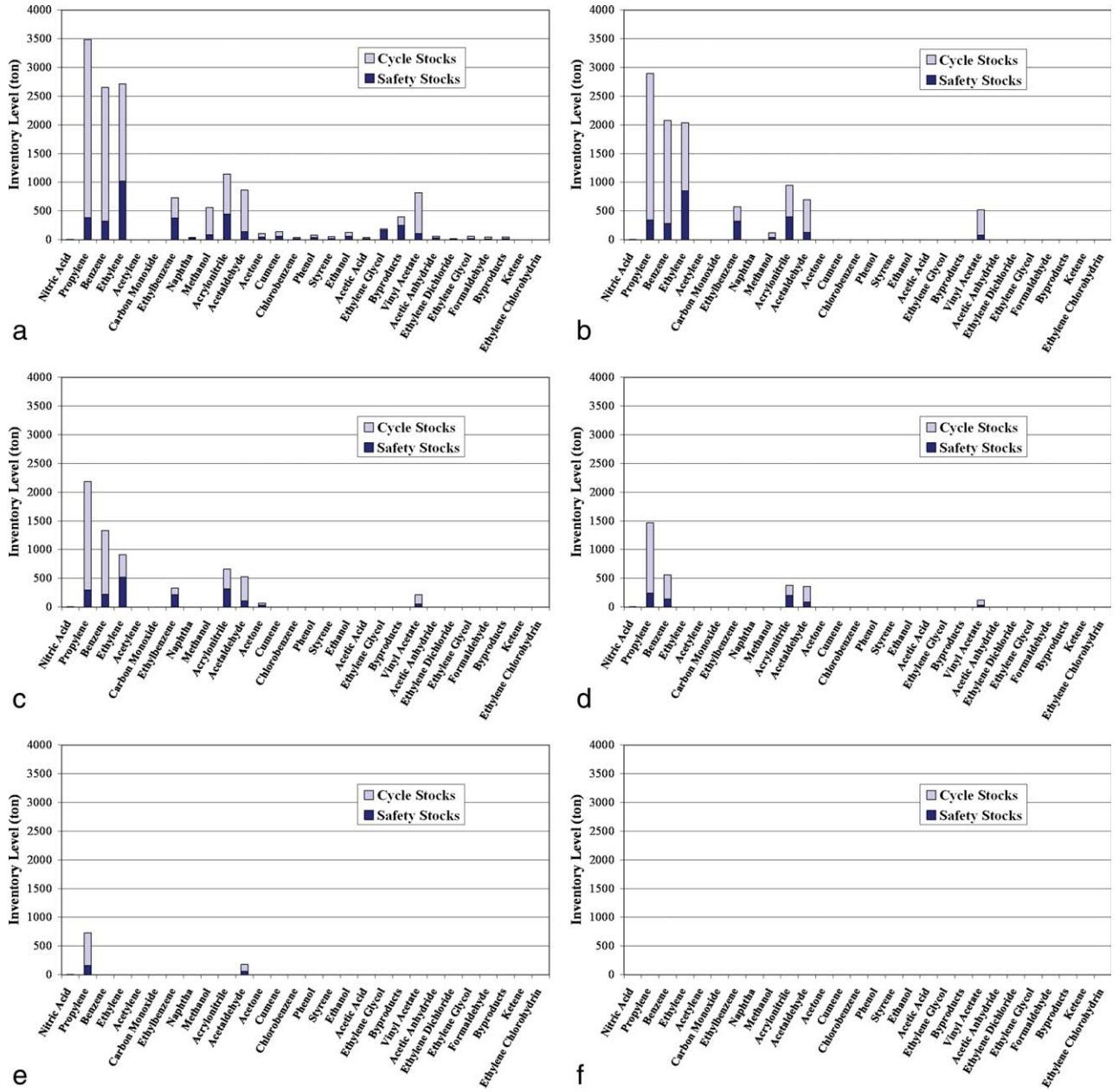

Figure 20. Optimal inventory levels of all the chemicals under different specifications of the maximum guaranteed service time to mark.

(a) Maximum guaranteed service time to the market is 0 day, (b) maximum guaranteed service time to the market is 10 days, (c) maximum guaranteed service time to the market is 20 days, (d) maximum guaranteed service time to the market is 30 days, (e) maximum guaranteed service time to the market is 40 days, and (f) Optimal inventory levels of all the chemicals for Example 5 when maximum guaranteed service time to the market is 50 days. [Color figure can be viewed in the online issue, which is available at wileyonlinelibrary.com.]

of this chemical process network. In addition, there are some inventories for other feedstocks and intermediates, but very few stocks for the final products. Particularly, the optimal inventory levels of acetylene, carbon monoxide, ketene, and ethylene chlorohydrin are zero in this case. When the maximum GST to the markets increases to 10 days, the optimal inventory levels for most chemicals decreases to zero, although there are still significant inventories for propylene, benzene, and ethylene, and a few stocks for nitric acid, ethylbenzene, naphtha, methanol, acrylonitrile, acetaldehyde, and vinyl acetate. If the maximum GST to the markets further increases to 20 days, the optimal inventory level of methanol decreases to zero. When the maximum GST to the markets equals to 40 days, we only need to hold inventory for nitric acid, propylene, and acetaldehyde. The optimal inventory levels of all the chemicals are zero when the maximum GST to the markets is 50 days.

Conclusions

In this article, we have developed an MINLP model to simultaneously optimize the inventory management decisions

and the mid-term process planning decisions for the production, purchase, and sale levels with the presence of supply and demand uncertainty. The guaranteed service approach is used to model the inventory system of a chemical complex, and the risk pooling effect is taken into account in the model by relating the probability distribution functions of the demands in the downstream nodes to their upstream nodes. Three illustrative examples are presented to demonstrate the applicability of the proposed model. To efficiently solve the resulting MINLP problem for large scale instances, we exploited some model properties and then proposed an efficient branch-and-refine algorithm based on successive piecewise linear approximation. Computational experiments on large-scale problems show that the proposed algorithm can obtain global optimal solutions very quickly without the need of a global optimizer.

A possible future extension is to integrate stochastic inventory management with the long-term process planning and take into account the optimal capacity planning of production process and storage facilities. The extension of the proposed framework to address multisite problems could be another future research direction.

Acknowledgments

The authors thank the financial support from the National Science Foundation under Grant No. DMI-0556090 and No. OCI-0750826, and Pennsylvania Infrastructure Technology Alliance (PITA). F. You is also grateful to Dr. John M. Wassick at The Dow Chemical Company for helpful discussions at the early stage of this work.

Notation

Sets/indices

I = set of processes indexed by i
J = set of chemicals indexed by j
K = set of external suppliers indexed by k
L = set of external markets indexed by l
M = set of integers for binary representation indexed by m
P = set of pieces for piecewise linear approximation indexed by p

Subsets

$i \in I(j)$ = the subset of processes that consume chemical j (for $\eta_{ij} > 0$)
$i \in O(j)$ = the subset of processes that produce chemical j (for $\eta_{ij} < 0$)
$j \in C_i$ = the subset of chemicals that are input of output of processes i
$j \in M_i$ = the subset of main products of processes i
$k \in \mathrm{SUP}(j)$ = the subset of external supplier k that supplies chemical j
$l \in \mathrm{MKT}(j)$ = the subset of external market l that has demand of chemical j

Parameters

λ_j = safety stock factor for chemical j
h_j = unit inventory holding cost of chemical j
Cap_i = total capacity of process i
δ_i = unit operating cost for process i
PD_i = production time delay of process i
η_{ij} = mass balance coefficient of chemical j for process i
$\overline{\mu}_{jl}$ = mean value of external demand of chemical j from the market l
$\overline{\sigma}_{jl}$ = standard deviation of external demand of chemical j to the market
$\overline{V}_{jl}$ = variance of external demand of chemical j from the market l
$\overline{R}_{jl}$ = variance to mean ratio for the demand of chemical j from market l ($\overline{R}_{jl} = \overline{\sigma}^2_{jl}/\overline{\mu}_{jl} = \overline{V}_{jl}/\overline{\mu}_{jl}$)
a^{L}_{jk} = lower bound for the availability of chemical j in the external supplier k
a^{U}_{jk} = upper bound for the availability of chemical j in the external supplier k
Γ_{jk} = price of purchase of chemical j from the supplier k
SI_{jk} = guaranteed service time (GST) for chemical j of external supplier k
$\mathrm{SO}^{\mathrm{U}}_{jl}$ = maximum service time for chemical j to external market l
γ_{ij} = deterministic transfer time from process i to storage tank of chemical j
θ_{ij} = deterministic transfer time from storage tank of chemical j to process i
M = the maximum positive value such that PD_i/M, SI_{jk}/M, $\mathrm{SO}^{\mathrm{U}}_{jl}/M$, γ_{ij}/M, and θ_{ij}/M are all integers
α_{jp} = piecewise linear approximation parameter, $\alpha_{j,p} = \frac{\sqrt{u_{j,p}} - \sqrt{u_{j,p-1}}}{u_{j,p} - u_{j,p-1}}$
β_{jp} = piecewise linear approximation parameter, $\beta_{jp} = \sqrt{u_{jp}} - \alpha_{jp} u_{jp}$
u_{jp} = parameters for the bounds of intervals in piecewise linear approximation

Binary variables (0-1)

X_{jk} = 0-1 variable. Equal to 1 if there is positive flow rate from external supplier k to the storage tank of chemical j
Y_{ijl} = 0-1 variable. Equal to 1 if the variance to mean ratio of raw materials of process i equal to the one of chemical j from market l
Z_{ijm} = 0-1 variable for the binary representation of the net lead time of chemical j for the demand from downstream process i
$E_{j,p}$ = auxiliary 0-1 variable for piecewise linear approximation

Continuous variables (0 to ∞)

SP_{ij} = guaranteed service time of process i to its downstream storage tank of chemical j
SC_{ij} = guaranteed service time of chemical j to its downstream process i
TC_j = worst case replenishment lead time of the storage tank for chemical j
TP_i = worst case replenishment lead time of process i
SO_{jl} = guaranteed service time of chemical j to external market l
N_{ij} = net lead time of chemical j for the demand from downstream process i
$\overline{N}_{jl}$ = net lead time of chemical j for the demand from external market l
V_{ij} = variance of internal demand of chemical j in process i
W_{ij} = amount of flow of chemical j to/from process i
Pu_{jk} = amount of chemical j purchased from external supplier k
Sa_{jl} = amount of chemical j sold to external market l
RC_j = the variance to mean ratio for all the demands of chemical j
RP_i = variance to mean ratio for the demands of input chemicals of process i

Auxiliary variables (0 to ∞)

$\mathrm{WY}_{i,j,l}$ = auxiliary variable, $\mathrm{WY}_{i,j,l} = W_{ij} \cdot Y_{i,j,l}$
$\mathrm{WY1}_{i,j,l}$ = auxiliary variable
G_j = auxiliary variable, $G_j = \sum_{l \in \mathrm{MKT}(j)} \bar{N}_{jl} \cdot \bar{V}_{jl} + \sum_{i \in I(j)} N_{ij} \cdot V_{ij}$.
Q_j = auxiliary variable, $Q_j = \sum_{l \in \mathrm{MKT}(j)} \bar{N}_{jl} \cdot \bar{W}_{jl} + \sum_{i \in I(j)} N_{ij} \cdot W_{ij}$
ZV_{ijm} = auxiliary variable, for the product of Z_{ijm} and V_{ij}
$\mathrm{ZV1}_{ijm}$ = auxiliary variable
F_{jp} = auxiliary variable for piecewise linear approximation

Literature Cited

1. Wassick JM. Enterprise-wide optimization in an integrated chemical complex. *Comput Chem Eng*. 2009;33:1950–1963.

2. Norton LC, Grossmann IE. Strategic planning model for complete process flexibility. *Ind Eng Chem Res*. 1994;33:69–76.
3. Sahinidis NV, Grossmann IE. Optimization model for the long range planning in the chemical industry. *Comput Chem Eng*. 1989;13:1049–1063.
4. Ierapetritou MG, Pistikopoulos EN, Floudas CA. Operational planning under uncertainty. *Comput Chem Eng*. 1996;20:1499–1516.
5. Jung JY, Blau G, Pekny JF, Reklaitis GV, Eversdyk D. Integrated safety stock management for multi-stage supply chains under production capacity constraints. *Comput Chem Eng*. 2008;32:2570–2581.
6. Liu ML, Sahinidis NV. Optimization in process planning under uncertainty. *Ind Eng Chem Res*. 1995;35:4154–4165.
7. Barbaro A, Bagajewicz MJ. Managing financial risk in planning under uncertainty. *AIChE J*. 2004;50:963–989.
8. Cheng L, Subrahmanian E, Westerberg AW. Design and planning under uncertainty: issues on problem formulation and solution *Comput Chem Eng*. 2003;27:781–801.
9. Pistikopoulos EN. Uncertainty in process design and operations. *Comput Chem Eng*. 1995;19:553–563.
10. You F, Grossmann IE. Design of responsive supply chains under demand uncertainty. *Comput Chem Eng*. 2008;32:2839–3274.
11. Zipkin PH. *Foundations of Inventory Management*. Boston, MA: McGraw-Hill, 2000.
12. Grossmann IE. Enterprise-wide optimization: a new frontier in process systems engineering. *AIChE J*. 2005;51:1846–1857.
13. Varma VA, Reklaitis GV, Blau GE, Pekny JF. Enterprise-wide modeling and optimization—an overview of emerging research challenges and opportunities. *Comput Chem Eng*. 2007;31:692–711.
14. Graves SC, Willems SP. Optimizing strategic safety stock placement in supply chains. *Manuf Serv Oper Manage*. 2000;2:68–83.
15. Graves SC, Willems SP. *Supply chain design: safety stock placement and supply chain configuration*. In: de Kok AG, Graves SC, editors. *Handbooks in Operations Research and Management Science*, *Vol*. 11. North-Holland, Amsterdam: Elsevier, 2003:95–132.
16. Graves SC, Willems SP. Optimizing the supply chain configuration for new products. *Manage Sci*. 2005;51:1165–1180.
17. Inderfurth K. Safety stock optimization in multi-stage inventory systems. *Int J Prod Econ*. 1991;24:103–113.
18. Eppen G. Effects of centralization on expected costs in a multi-echelon newsboy problem. *Manage Sci*. 1979;25:498–501.
19. You F, Castro PM, Grossmann IE. Dinkelbach's algorithm as an efficient method to solve a class of MINLP models for large-scale cyclic scheduling problems. *Comput Chem Eng*. 2009;33:1879–1889.
20. Jackson JR, Grossmann IE. Temporal decomposition scheme for nonlinear multisite production planning and distribution models. *Ind Eng Chem Res*. 2003;42:3045–3055.
21. Verderame PM, Floudas CA. Integrated operational planning and medium-term scheduling of a large-scale industrial batch plants. *Ind Eng Chem Res*. 2008;47:4845–4860.
22. Ierapetritou MG, Acevedo J, Pistikopoulos EN. An optimization approach for process engineering problems under uncertainty. *Comput Chem Eng*. 1996;20:703–709.
23. Bok J-K, Grossmann IE, Park S. Supply chain optimization in continuous flexible process networks. *Ind Eng Chem Res*. 2000;39:1279–1290.
24. Chen C-L, Lee W-C. Multi-objective optimization of multi-echelon supply chain networks with uncertain product demands and prices. *Comput Chem Eng*. 2004;28:1131–1144.
25. Gupta A, Maranas CD, McDonald CM. Mid-term supply chain planning under demand uncertainty: customer demand satisfaction and inventory management. *Comput Chem Eng*. 2000;24:2613–2621.
26. Ierapetritoua MG, Pistikopoulosa EN, Floudas CA. Operational planning under uncertainty. *Comput Chem Eng*. 1996;20:1499–1516.
27. Neiro SMS, Pinto JM. A general modeling framework for the operational planning of petroleum supply chains. *Comput Chem Eng*. 2004;28:871–896.
28. You F, Grossmann IE. *Optimal design and operational planning of responsive process supply chains*. In: Papageorgiou LG, Georgiadis MC, editors. *Process System Engineering*, *Vol*. 3: *Supply Chain Optimization*. Weinheim: Wiley-VCH, 2007:107–134.
29. You F, Wassick JM, Grossmann IE. Risk management for global supply chain planning under uncertainty: models and algorithms. *AIChE J*. 2009;55:931–946.
30. Simpson KF. In-process inventories. *Oper Res*. 1958;6:863–873.
31. Clark A, Scarf S. Optimal policies for a multi-echelon inventory problem. *Manage Sci*. 1960;6:475–490.
32. Humair S, Willems SP. Optimizing strategic safety stock placement in supply chains with clusters of commonality. *Oper Res*. 2006;54:725–742.
33. Magnanti TL, Shen Z-JM, Shu J, Simchi-Levi D, Teo C-P. Inventory placement in acyclic supply chain networks. *Oper Res Lett*. 2006;34:228–238.
34. Shu J, Karimi IA. Efficient heuristics for inventory placement in a cyclic networks. *Comput Oper Res*. 2009;36:2899–2904.
35. You F, Grossmann IE. Mixed-integer nonlinear programming models and algorithms for large-scale supply chain design with stochastic inventory management. *Ind Eng Chem Res*. 2008;47:7802–7817.
36. You F, Grossmann IE. Integrated multi-echelon supply chain design with inventories under uncertainty: MINLP models, computational strategies. *AIChE J*. 2008;56:419–440.
37. You F, Grossmann IE. Balancing responsiveness and economics in the design of process supply chains with multi-echelon stochastic inventory. *AIChE J*. In press. DOI: 10.1002/aic.12244
38. Graves SC. Safety stocks in manufacturing systems. *J Manuf Oper Manage*. 1988;1:67–101.
39. Inderfurth K, Minner S. Safety stocks in multi-stage inventory systems under different service measures. *Eur J Oper Res*. 1998;106:57–73.
40. Kondili E, Pantelides CC, Sargent RWH. General algorithm for short-term scheduling of batch operations. I. Milp formulation. *Comput Chem Eng*. 1993;17:211–227.
41. Floudas CA, Aggarwal A. A decomposition strategy for global optimum search in the pooling problem. *ORSA J Comput*. 1990;2:225–235.
42. Lee HL, Padmanabhan V, Whang S. The bullwhip effect in supply chains. *Sloan Manage Rev*. 1997;38:93–102.
43. Sahinidis NV. BARON: a general purpose global optimization software package. *J Global Optim*. 1996;8:201–205.
44. Brooke A, Kendrick D, Meeraus A, Raman R. *GAMS—A User's Manual*. Washington, DC: GAMS Development Corp., 1998.
45. Iyer RR, Grossmann IE. A bilevel decomposition algorithm for long-range planning of process networks. *Ind Eng Chem Res*. 1998;37:474–481.
46. Minner S. Strategic safety stocks in reverse logistics supply chains. *Int J Prod Econ*. 2001;71:417–428.
47. Falk JE, Soland RM. An algorithm for separable nonconvex programming problems. *Manage Sci*. 1969;15:550–569.
48. Schectman JP, Sahinidis NV. A finite algorithm for global minimization of separable concave programs. *J Global Optim*. 1998;12:1–36.
49. Nemhauser GL, Wolsey LA. *Integer and Combinatorial Optimization*. New York, NY: Wiley, 1988.
50. Glover F. Improved linear integer programming formulations of nonlinear integer problems. *Manage Sci*. 1975;22:455–460.
51. Bergamini ML, Grossmann IE, Scenna N, Aguirre P. An improved piecewise outer-approximation algorithm for the global optimization of MINLP models involving concave and bilinear terms. *Comput Chem Eng*. 2008;32:477–493.
52. Croxton KL, Gendron B, Magnanti TL. A comparison of mixed-integer programming models for nonconvex piecewise linear cost minimization problems. *Manage Sci*. 2003;49:1268–1273.
53. Padberg MW. Approximating separable nonlinear functions via mixed zero-one programs. *Oper Res Lett*. 2000;27:1–5.
54. Wicaksono DS, Karimi IA. Piecewise MILP under- and overestimators for global optimization of bilinear programs. *AIChE J*. 2008;54:991–1008.

Manuscript received Jan. 21, 2010, revision received Apr. 1, 2010, and final revision received Jun. 18, 2010.